



## Longitudinal detection of subcategorized CD44v6<sup>+</sup> CTCs and circulating tumor endothelial cells (CTECs) enables novel clinical stratification and improves prognostic prediction of small cell lung cancer: A prospective, multi-center study

Ying Wang<sup>a,1</sup>, Lina Zhang<sup>b,1</sup>, Jinjing Tan<sup>b,1</sup>, Zhiyun Zhang<sup>b</sup>, Yanxia Liu<sup>b</sup>, Xingsheng Hu<sup>c</sup>, Baohua Lu<sup>a</sup>, Yuan Gao<sup>a</sup>, Li Tong<sup>a</sup>, Zan Liu<sup>a</sup>, Hongxia Zhang<sup>d</sup>, Peter Ping Lin<sup>e</sup>, Baolan Li<sup>a</sup>, Olivier Gires<sup>f,\*\*</sup>, Tongmei Zhang<sup>a,\*</sup>

<sup>a</sup> Department of Medical Oncology, Beijing Chest Hospital, Capital Medical University, Beijing Tuberculosis and Thoracic Tumor Research Institute, Beijing, China

<sup>b</sup> Department of Cancer Research Center, Beijing Chest Hospital, Capital Medical University, Beijing Tuberculosis and Thoracic Tumor Research Institute, Beijing, China

<sup>c</sup> Department of Medical Oncology, National Cancer Center/National Clinical Research Center for Cancer/Cancer Hospital, Chinese Academy of Medical Sciences & Peking Union Medical College, Beijing, China

<sup>d</sup> Department of Respiratory and Critical Care Medicine, Beijing Luhe Hospital, Capital Medical University, Beijing, China

<sup>e</sup> Cytelligen, San Diego, CA, USA

<sup>f</sup> Department of Otorhinolaryngology, Head and Neck Surgery, University Hospital, LMU, Munich, Germany

### ARTICLE INFO

#### Keywords:

Aneuploid CTCs and CTECs  
SE-iFISH  
Treatment response  
Metastasis  
Prognosis

### ABSTRACT

Current management of small cell lung cancer (SCLC) remains challenging. Effective biomarkers are needed to subdivide patients presenting distinct treatment response and clinical outcomes. An understanding of heterogeneous phenotypes of aneuploid CD31<sup>+</sup> circulating tumor cells (CTCs) and CD31<sup>+</sup> circulating tumor endothelial cells (CTECs) may provide novel insights in the clinical management of SCLC. In the present translational and prospective study, increased cancer metastasis-related cell proliferation and motility, accompanied with up-regulated mesenchymal marker vimentin but down-regulated epithelial marker *E-cadherin*, were observed in both lentivirus infected SCLC and NSCLC cells overexpressing the stemness marker CD44v6. Aneuploid CTCs and CTECs expressing CD44v6 were longitudinally detected by SE-iFISH in 120 SCLC patients. Positive detection of baseline CD44v6<sup>+</sup> CTCs and CD44v6<sup>+</sup> CTECs was significantly associated with enhanced hepatic metastasis. Karyotype analysis revealed that chromosome 8 (Chr8) in CD44v6<sup>+</sup> CTCs shifted from trisomy 8 towards multiploidy in post-therapeutic patients compared to pre-treatment subjects. Furthermore, the burden of baseline CD44v6<sup>+</sup> CTCs (t<sub>0</sub>) or amid the therapy (t<sub>1-2</sub>), the ratio of baseline CD31<sup>+</sup> CTEC/CD31<sup>+</sup> CTC (t<sub>0</sub>), and CTC-WBC clusters (t<sub>0</sub>) were correlated with treatment response and distant metastases, particularly brain metastasis, in subjects with limited disease (LD-SCLC) but not in those with extensive disease (ED-SCLC). Multivariate survival analysis validated that longitudinally detected CD44v6<sup>+</sup>/CD31<sup>+</sup> CTCs was an independent prognostic factor for inferior survival in SCLC patients. Our study provides evidence for the first time that comprehensive analyses of CTCs, CTECs, and their respective CD44v6<sup>+</sup> subtypes enable clinical stratification and improve prognostic prediction of SCLC, particularly for potentially curable LD-SCLC.

\* Corresponding author. Department of Medical Oncology, Beijing Chest Hospital, Capital Medical University & Beijing Tuberculosis and Thoracic Tumor Research Institute. NO.9 Beiguan Street, Tongzhou District, Beijing 101149, China

\*\* Corresponding author.

E-mail addresses: [olivier.gires@med.uni-muenchen.de](mailto:olivier.gires@med.uni-muenchen.de) (O. Gires), [tongmeibj@ccmu.edu.cn](mailto:tongmeibj@ccmu.edu.cn) (T. Zhang).

<sup>1</sup> These authors contributed equally to this work.

## 1. Introduction

Small cell lung cancer (SCLC) is the most lethal lung cancer subtype worldwide, characterized by progressive growth, early distant metastases, and rapidly acquired therapeutic resistance [1,2]. Despite decades of studies [3,4], prognosis of SCLC patients remains exceedingly poor, with a five-year survival rate below 7% [5]. In clinical practice, surgical resection is only recommended for patients with clinical stages T1-2N0M0, which account for less than 5% of total SCLC cases [6,7]. Initial treatment strategy for most patients is primarily derived based on the Veterans Administration Lung Cancer Study Group (VALSG) staging system, which simply categorizes SCLC into limited disease (LD)- and extensive disease (ED)-SCLC [8]. However, this image-based division inevitably ignores tumor heterogeneity and micrometastatic burden in tumors with the same disease stage [9]. Hence, treatment-resistant patients are poorly characterized and clinical outcomes in patients with identical stages can substantially vary [10–12]. Until recently, identification of practical, non-invasive biomarkers for guiding the management of SCLC patients in clinical practice has been unsuccessful [13].

Liquid biopsy [14–17], involving detection and analysis of circulating tumor cells (CTCs) [18,19] and circulating tumor endothelial cells (CTECs) [20,21] which derive from CD31<sup>+</sup> tumor endothelial cells (TECs), is a useful non-invasive diagnostic tool to represent tumor heterogeneity and to dynamically monitor tumor progression. One of the most distinctive characteristics of TECs is the chromosomal aneuploidy [22], the hallmark of neoplastic cells. Comparing to normal ECs, TECs revealed transcriptomic differences [23]. Aneuploid TECs and CTECs likely develop from “cancerization of stromal endothelial cells” and/or “endothelialization of tumor cells” in the hypoxic tumor microenvironment [21]. Both aneuploid CD31<sup>-</sup> CTCs and CD31<sup>+</sup> CTECs mirror tumor heterogeneity and progression. Molecular characteristics of CTCs and CTECs may either evolve or become selected to facilitate metastasis and create therapeutic resistance during disease progression [24–26]. Though increasing evidence has established the prognostic value of quantified CTCs in lung cancer [14,27,28], few reports have described the heterogeneity, evolutionary and/or selection-related changes of CTCs and CTECs against stressful treatment regimens during disease progression in SCLC. Furthermore, the landscape and clinical significance of SCLC CTCs and CTECs’ subpopulations possessing distinct phenotypes remain to be elucidated.

CD44v6, a specific CD44 variant isoform (CD44v), is a critical stem cell marker with reported repercussions for therapeutic resistance, tumor metastasis, and disease progression [29,30]. Expression of CD44 on tumor cells has been documented elsewhere and has received considerable attention [31,32], CTCs and CTECs expressing CD44 are more likely to escape from immunological surveillance, enhancing tumor recurrence and metastasis [33–36]. However, the functional and clinical significance of CD44v6<sup>+</sup> CTCs and CTECs in SCLC is still unclear.

Herein, extending beyond our previous study on EpCAM<sup>+</sup> and/or Vimentin<sup>+</sup> CTCs and CTECs in non-small cell lung cancer (NSCLC) patients subjected to anti-angiogenic bevacizumab treatment [37,38], we report the existence of a full spectrum of CTCs and CTECs longitudinally detected in SCLC patients undergoing disease stage-based standard treatment. A comprehensive analysis was performed to explore the clinical significance of aneuploid CD31<sup>-</sup> CTCs, CD31<sup>+</sup> CTECs, and their CD44v6-expressing subpopulations.

## 2. Materials and methods

### 2.1. *In vitro* functional assays of CD44v6 in lung cancer cell line cells

#### 2.1.1. Cell lines and cell culture

Two adherent SCLC cell lines (DMS114 and H446) and two NSCLC cell lines (A549 and H1299) were obtained from the National Infrastructure of Cell Line Resource (Beijing, China). Cells were cultured in RPMI 1640 medium (Life Technologies, Grand Island, NY, USA)

supplemented with 10% fetal bovine serum (FBS) and 1% antibiotic-antimycotic solution (Sigma-Aldrich, St. Louis, MO, USA). All cells were maintained at 37 °C in humidified air with 5% CO<sub>2</sub>.

#### 2.1.2. RNA extraction and quantitative reverse transcription PCR

Total mRNA was extracted from cells with TRIzol reagent (Invitrogen, Carlsbad, CA, USA), and 1 µg RNA was used for reverse transcription with First-strand cDNA transcription kit (TransGen Biotech, Beijing, China) according to the manufacturer’s instructions. Real-time PCR analysis of CD44 standard isoform (CD44s) and CD44v6 expression was conducted with the following primers: CD44s-Forward 5'-GGAGCAGCACTTCAGGAGGTTAC-3', CD44s-Reverse 5'-GGAATGTGTCTTGGTCTCTGGTAGC-3', CD44v6-Forward 5'-CCAGGCAACTCCTAGTAGTACAA CG-3' and CD44v6-Reverse 5'-CGAATGGGAGTCTTCTTTGGGT-3'. The housekeeping gene β-actin was used as an internal control, with the primers as β-actin-Forward 5'-GTGAAGGTGACAGCAGTCGGTT-3' and β-actin-Reverse 5'-GAAGTGGGGTGGCTT TTAGGAT-3'. A SYBR® Green Master Mix Kit (ThermoFisher, CA, USA) was used for real-time PCR analysis with standard amplification protocol. The 2<sup>-ΔΔCT</sup> (where CT is the threshold cycle) method was used to determine the fold change in gene transcription. Each sample was performed in triplicate and experiments were repeated three times.

#### 2.1.3. Construction of the recombinant lentiviral vector and infection into cell lines

Recombinant lentiviral vectors were designed and packaged in 293 T cells by GeneChem (Shanghai, China). For cellular infection, cells were subcultured in 96-well culture plate and infected with lentivirus either packaged with CD44v6 overexpression (CD44v6<sup>OE</sup>) vector or the vector alone as a negative control (NC). Stably infected clones were selected by puromycin.

#### 2.1.4. Cell proliferation assay

Cell proliferation rates were measured using Cell Counting Kit 8 (CCK8, Dojindo Laboratories, Tokyo, Japan). Briefly, 3000 tumor cells of each group were seeded into 96-well plates in 100 µL of culture medium. For every 12 h or 24 h, the culture medium was changed to CCK-8 solution (110 µL/well), followed by incubation for another 2 h. The optical density (OD) was measured at 450 nm with a microplate reader (BioTek Synergy HT, Winooski, VT, USA). The assay was repeated three times and the data are presented as the mean ± standard error of the readouts.

#### 2.1.5. Wound scratch assay

Cells were plated in a 6-well plate and cultured overnight before serum starvation for 24 h. After scratching with a pipette tip, wounds were observed and recorded at every 18 h along the scratch. Cell migration ability was expressed as the migration speed of cells from each wound edge reached.

#### 2.1.6. Cell migration assay

The migration assay was performed in a 24-well transwell plate containing a polycarbonate membrane-coated chamber with an 8.0 µm size pore. For migration assay, after starvation for 24 h, 6 × 10<sup>4</sup> cells in 100 µL serum-free medium were added to the upper compartment of the chamber, while the lower compartment was filled with 600 µL of RPMI 1640 supplemented with 10% FBS. After incubation at 37 °C for 24 h, cells on the lower surface of the membrane were fixed and stained with 2% crystal violet. The number of cells on the lower surface of the membrane was counted in five microscopic fields at 200 × magnification.

#### 2.1.7. Western blot analysis

Briefly, total proteins of cell extracts were separated using 10% Sodium Dodecyl Sulfate-Poly Acrylamide Gel Electrophoresis (SDS-PAGE) and then transferred onto nitrocellulose membranes. After blocking with

5% skim milk, membranes were incubated with designated primary antibodies overnight at 4 °C, followed by incubation with HRP conjugated second antibody for 3 h at 4 °C. Proteins were visualized using ECL reagent (Abclonal, China).

## 2.2. Participants and study design

A prospective, non-interventional, multi-centric study was conducted at three medical centers in China (Beijing Chest Hospital, Capital Medical University; Cancer Hospital, Chinese Academy of Medical Sciences and Peking Union Medical College; Beijing Luhe Hospital, Capital Medical University). The study design and workflow diagram are shown in Fig. 2. All patients were histologically or cytologically confirmed, and the clinical stage was determined by brain magnetic resonance imaging (MRI), computed tomography (CT) of the chest and abdomen, radio-nuclide bone scanning, or positron emission tomography (PET) scanning. Briefly, patients aged 18–75 years old with treatment-naïve, pathologically diagnosed unresectable SCLC and those with a performance status (PS) of 0–2, with adequate organ function and evaluable tumor lesions, were eligible for this study. Patients with a history of other malignant tumors were excluded.

A total of 124 patients were prospectively enrolled from January 2018 to January 2020, and 120 patients who received standard first-line platinum-based chemotherapy alone or plus concurrent or sequential radiotherapy were ultimately eligible for final analysis. Six weeks (two cycles) after treatment initiation, clinical response was evaluated employing standard radiography according to Response Evaluation Criteria in Solid Tumors (RECIST) version 1.1 criteria. Responses were recorded as partial response (PR), progressive disease (PD), or stable disease (SD). A total of 245 samples were collected from a cohort of 120 patients (see sample collection flow chart in Supplementary Fig. S1). Peripheral blood (PB) was periodically collected prior to chemotherapy administration ( $t_0$ ), after two cycles of chemotherapy ( $t_1$ ), and post-four-to-six treatment cycles ( $t_2$ ). The relationship between baseline CD44v6<sup>+</sup> CTCs and CTECs with patients' characteristics was evaluated. Moreover, the correlation of correlation of CTC and CTEC-relevant variables with clinical factors was investigated in LD- and ED-SCLC patients separately. Univariate and multivariate analyses were applied to evaluate the prognostic significance of CD44v6<sup>+</sup> CTCs in SCLC patients. This study was conducted in accordance with the Declaration of Helsinki Principles. All patients provided written informed consent. Blood sample collection was conducted according to the protocols approved by the Ethics and Scientific Committee of Beijing Chest Hospital (No. BJXKYY 201802-01).

## 2.3. SE-iFISH

Subtraction enrichment and immunostaining-fluorescence in situ hybridization (SE-iFISH) was performed according to a previously published protocol (Cytelligen, San Diego, CA, USA) with minor modifications [39]. Briefly, 6 ml of blood, which were collected into a tube containing ACD anti-coagulant (Becton Dickinson, Franklin Lakes, NJ, USA) and stored at room temperature for no more than 48 h, were centrifuged at 200×g for 15 min at room temperature to deplete supernatant plasma. Sedimented blood cells were resuspended with 3 ml hCTC buffer and loaded on the top of a non-hematologic cell separation matrix in a 50 ml tube. Samples were centrifuged at 450×g for 5 min, followed by collection of liquid fraction above red blood cells (RBCs). This fraction containing WBCs was then incubated with immuno-magnetic beads conjugated to a mix of anti-leukocyte monoclonal antibodies at room temperature for 20 min with gentle shaking. WBCs-bound immuno-beads were depleted using a magnetic separator suitable for 50 ml tubes (Cytelligen). The remaining non-hematologic cells were thoroughly mixed with cell fixative, smeared on formatted CTC slides, and dried for subsequent iFISH processing.

Modified six-color iFISH was performed as previously described

[39]. Coated slides containing dried monolayer cells were rinsed with PBS, followed by dehydration and subsequent FISH hybridization with the chromosome 8 centromere probe (CEP8 Spectrum Orange, Vysis, Abbott Laboratories, Chicago, IL, USA) for 3 h utilizing a ThermoBrite FISH Slides Processing System (Leica Biosystems, Buffalo Grove, IL, USA). Samples were subsequently incubated with indicated monoclonal antibodies, including Alexa Fluor (AF)594-anti-CD45 (Clone 9.4), AF488-anti-CD44v6 (Clone REA706), Cy5-anti-CD31 (Clone WM59), and Cy7-anti-Vimentin (Clone 1D3) at room temperature for 20 min in the dark. After washing, the iFISH Full Spectrum Anti-Fade Mounting Medium containing DAPI (Cytelligen, San Diego, CA, USA) which effectively protects the full spectrum fluorescence staining from fading was added to the samples prior to be subjected to the automated imaging system. Conjugation of all different fluorescent dyes to the applied antibodies was performed in-house at Cytelligen.

## 2.4. Automated CTC 3D scanning and image analysis with Metafer-iFISH

CTC slides were automatically scanned and analyzed with the Metafer-iFISH imaging system co-developed by Carl Zeiss (Oberkochen, Germany), MetaSystems (Altussheim, Germany), and Cytelligen. Cells on the slide were subjected to 3D scanning with cross Z-sectioning at 1 μm-steps of depth in each fluorescence channel. Identification criteria for CTCs included: DAPI<sup>+</sup>/CD45<sup>-</sup>/CD31<sup>-</sup>/CD44v6<sup>±or-</sup>/Vim<sup>±or-</sup> aneuploid cells and DAPI<sup>+</sup>/CD45<sup>-</sup>/CD31<sup>-</sup>/CD44v6<sup>+</sup> or Vim<sup>+</sup> diploid/near-diploid cells. Criteria for CD31<sup>+</sup> CTECs included: DAPI<sup>+</sup>/CD45<sup>-</sup>/CD31<sup>+</sup>/CD44v6<sup>±or-</sup>/Vim<sup>±or-</sup> aneuploid cells and DAPI<sup>+</sup>/CD45<sup>-</sup>/CD31<sup>+</sup>/CD44v6<sup>+</sup> or Vim<sup>+</sup> diploid/near-diploid cells. Small cell: ≤5 μm; large cell: >5 μm. A cell cluster was defined as more than two individual cells with adjacent nuclei staying together. Comprehensive characterization and subcategorization of aneuploid CTCs and CTECs were performed on cell size, tumor marker expression, and the degree of aneuploidy.

## 2.5. Statistical analysis

All statistical analyses were conducted using SPSS 25.0 software (Chicago, IL, USA). The Chi-square and Fisher's exact tests were used to compare categorical data. Comparisons of continuous variables between groups were performed using the Mann-Whitney test. X-tile software was applied to determine the optimal cut-off value of CTCs. PFS was defined as the time from initial blood collection until disease progression or last follow-up. OS was defined as the time from initial blood collection until death or last follow-up. Kaplan-Meier survival plots for PFS or OS were generated based on diverse subtypes of CTCs, and the survival curves were compared using log-rank tests. A neural network-based algorithm was applied to comprehensively evaluate a series of variables' contributions to prognosis prediction. Uni- and multi-variate Cox proportional hazards regression models with HR and 95% CIs were applied to determine the independent prognostic factors for PFS and OS. All *p* values were two-sided, \**p* < 0.05, \*\**p* < 0.01 and \*\*\**p* < 0.001 are considered statistically significant, very significant, and extremely significant respectively in the following data.

## 3. Results

### 3.1. Overexpressed CD44v6 promotes SCLC and NSCLC cells migration and metastasis in vitro

To investigate the role of CD44v6 in tumor cell metastasis, two adherent SCLC cell lines, DMS114 and H446, stably overexpressing CD44v6 and negative control (NC) cells were developed through lentivirus infection (Fig. 1Aa-b). Compared to NC cells, increased CD44v6 protein expression in CD44v6<sup>OE</sup> cells was observed in Fig. 1Ba. As shown in Fig. 1Ca-b, increased expression of CD44v6 enhanced cell

proliferation in H446 cells though not in DMS114. The function of CD44v6 in regulating cancer cell motility was determined by wound scratch and transwell assays, the migration ability of both DMS114 and H446 cells was promoted by CD44v6 overexpression (Fig. 1Da-b and Fig. 1E).

We also performed CD44v6 overexpression in two NSCLC cell lines, A549 and H1299 (Fig. 1Ac-d), similar result demonstrated the increased

CD44v6 protein expression in CD44v6<sup>OE</sup> cells compared to NC cells in Fig. 1Bb. Increased expression of CD44v6 up-regulated the cell growth activity of A549 cells (Fig. 1Cc) but did not change cell growth in H1299 cells (Fig. 1Cd). As depicted in the wound scratch assay, the migration ability of A549 and H1299 cells was promoted in CD44v6<sup>OE</sup> group than the NC group (Fig. 1Dc-d). In the transwell assay, more A549-CD44v6<sup>OE</sup> cells crossed the membrane than A549-NC cells (Fig. 1E).

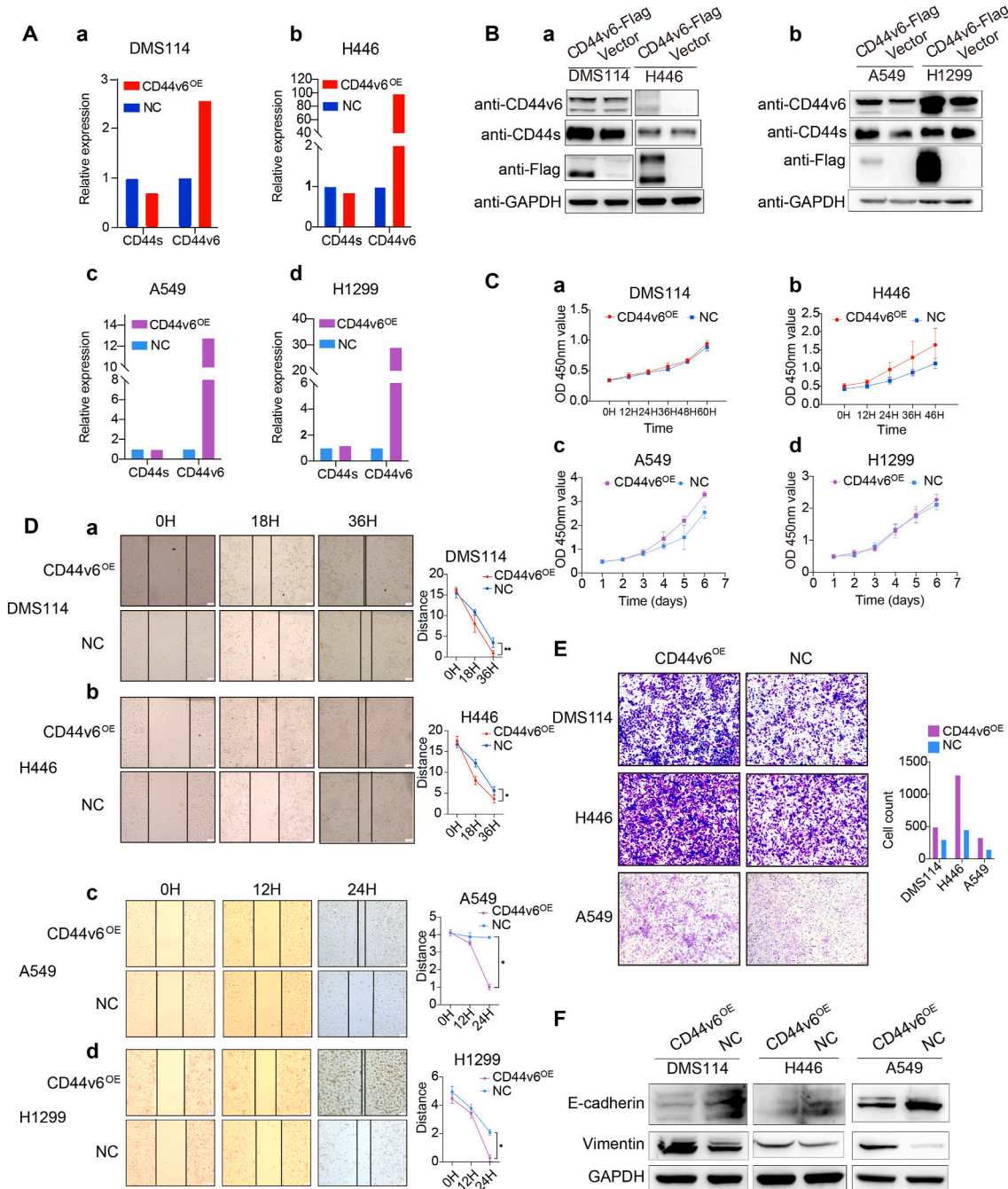


**Fig. 1. CD44v6 promoted SCLC and NSCLC cells metastasis in vitro.**

(Aa-d) Quantification of CD44s and CD44v6 mRNA in lentivirus infected SCLC cell line DMS114, H446 and NSCLC cell line A549 and H1299 cells. Increased CD44v6 mRNA is observed in CD44v6<sup>OE</sup> (overexpression, OE) cells but not in negative control (NC) cells. (Ba-b) Examination of CD44v6 protein in DMS114, H446, A549, H1299<sup>OE</sup> and NC cells. Compared to NC cells, increased CD44v6 protein expression in CD44v6<sup>OE</sup> cells is observed. (Ca-d) CCK8 proliferation assays. Measurement was performed on DMS114, H446, A549 and H1299 cells at 12 h intervals. The data are demonstrated as the mean ± standard error of the readouts from three separate experiments. (Da-d) Wound healing assay was performed on CD44v6 overexpressed cells as indicated. Increased cell motility is revealed in CD44v6 overexpressed cells. The distance between each edge of the cells was measured at each timepoint. \**p* < 0.05, \*\**p* < 0.01, *t*-test. (E) Cell migration assay. Cells migrated through the chamber are quantified and illustrated in histogram. (F) Examination of EMT related proteins. Compared to NC cells, reduced *E-cadherin* and increased *vimentin* in CD44v6<sup>OE</sup> cells are illustrated. *GAPDH* is the loading control.

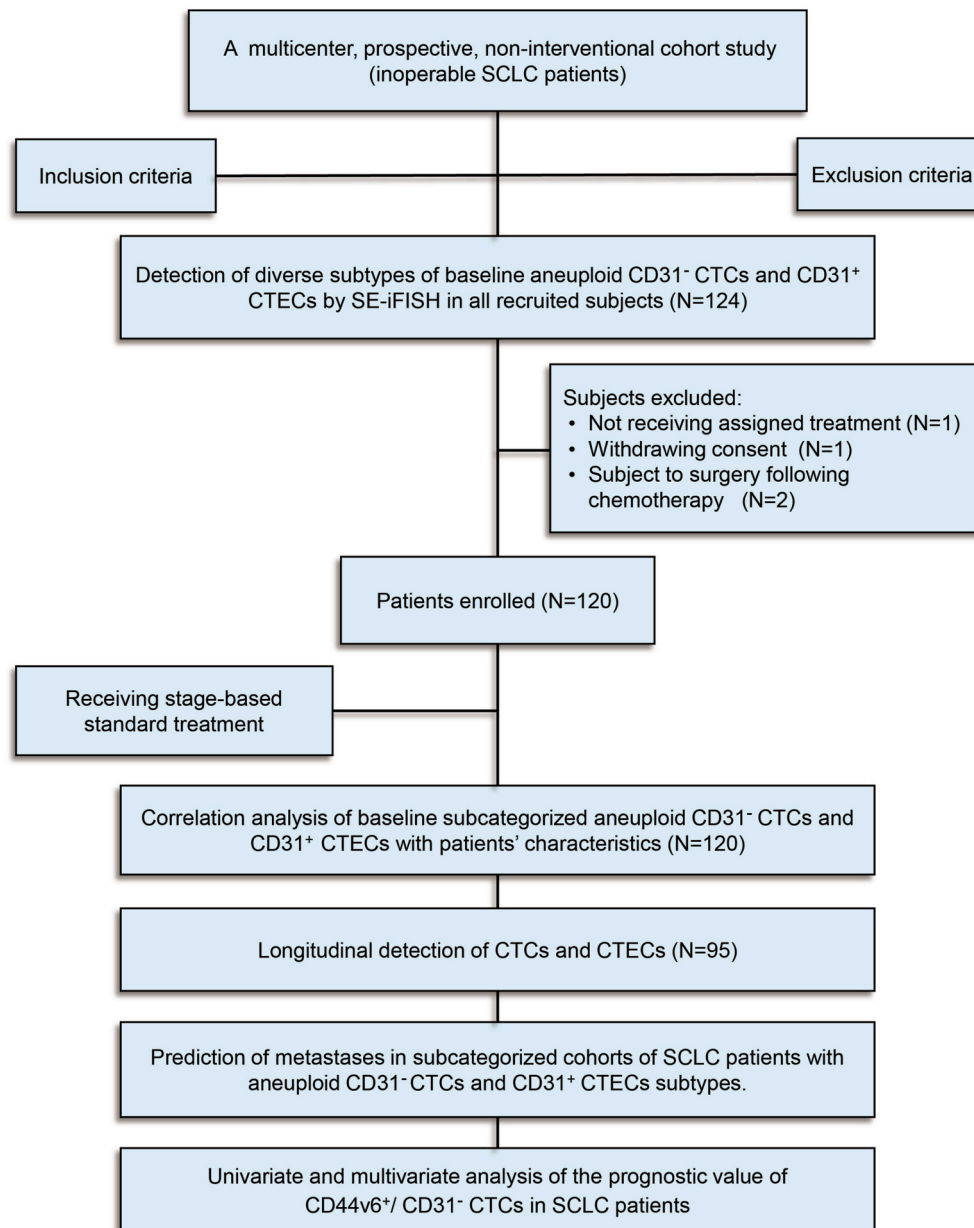


**Fig. 2.** Study design and workflow diagram.

Epithelial-mesenchymal cell transformation (EMT) is an essential process in cancer cell metastasis, featured by decreased intracellular adhesion and increased mobility. The protein expression levels of several EMT markers were evaluated by Western blot analysis in the current study. As depicted in Fig. 1F, the amount of the epithelial marker *E-cadherin* was reduced while the mesenchymal marker vimentin was increased in CD44v6<sup>OE</sup> group compared with NC group in both DMS114 and H446 cells. Similar experiment was conducted in A549 cells and result was consistent with SCLC cell lines (Fig. 1F). Collectively, these findings indicated that CD44v6 may promote cell invasion and migration through the activation EMT process, resulting in enhanced cancer metastases.

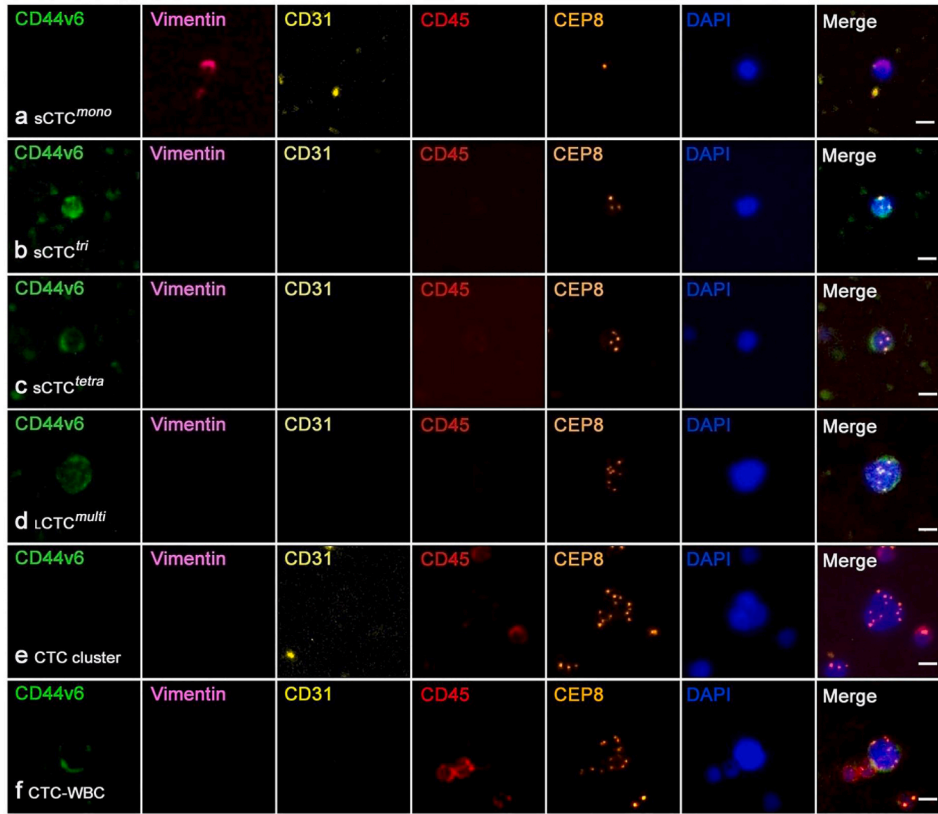
### 3.2. Co-detection of diverse subtypes of CTCs and CTECs in SCLC patients

Phenotypic and karyotypic characterization of different subtypes of aneuploid CTCs and CTECs was performed in 120 SCLC patients using SE-iFISH (Fig. 2). The cohort was composed of almost evenly distributed

LD-SCLC ( $n = 55$ ) and ED-SCLC cases ( $n = 65$ ). Samples from these patients covered baseline ( $t_0$ ) and post-treatment blood draws ( $t_1$  and  $t_2$ ). Ninety-five patients received longitudinal CTC detection. (Supplementary Fig. S1).

Diverse subtypes of CTCs and CTECs, classified upon heterogeneous cell size, degree of aneuploidy, and expression of CD44v6 or Vimentin, were observed in patients throughout therapy (Fig. 3). As shown in Fig. 3Aa-f, CTCs exhibited different degrees of aneuploidy, heterogeneous morphologies, and phenotypes, including small ( $\leq 5$  mm WBC) CD44v6<sup>-</sup>/Vim<sup>+</sup>/CD31<sup>-</sup> haploid CTCs ( $\zeta$ CTC<sup>mono</sup>, Fig. 3Aa), CD44v6<sup>+</sup>/Vim<sup>-</sup>/CD31<sup>-</sup> triploid and tetraploid CTCs ( $\zeta$ CTC<sup>tri</sup>, SCTCtetra, Fig. 3Ab-c), as well as large ( $> 5$  mm) CD44v6<sup>+</sup>/Vim<sup>-</sup>/CD31<sup>-</sup> multiploid ( $\geq$  pentasomy 8) CTCs ( $\zeta$ CTC<sup>multi</sup>, Fig. 3Ad) cells. A homotypic CTC cluster consisting of three CD44v6<sup>-</sup>/Vim<sup>-</sup>/CD31<sup>-</sup> multiploid null cells (Fig. 3Ae) and a heterotypic CTC-WBC cluster comprising a large CD44v6<sup>+</sup>/Vim<sup>-</sup>/CD31<sup>-</sup> multiploid CTC and two CD45<sup>+</sup> WBCs (Fig. 3Af) are also shown. Large CTECs included CD44v6<sup>-</sup>/Vim<sup>+</sup>/CD31<sup>+</sup> diploid ( $\zeta$ CTEC<sup>di</sup>, Fig. 3Ba), CD44v6<sup>+</sup>/Vim<sup>+</sup>/CD31<sup>+</sup> triploid ( $\zeta$ CTEC<sup>tri</sup>, Fig. 3Bb),

A CD31<sup>-</sup> CTC



B CD31<sup>+</sup> CTEC

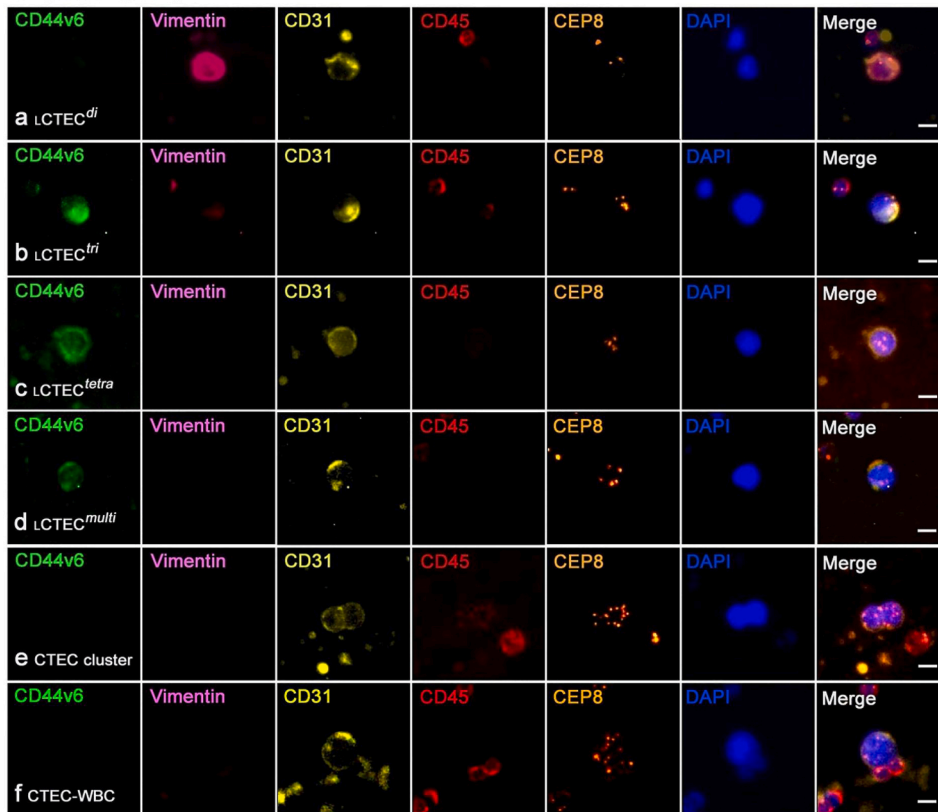


**Fig. 3.** Co-detection of diverse subtypes of aneuploid CD31<sup>-</sup> CTCs and CD31<sup>+</sup> CTECs expressing CD44v6 and/or Vimentin by SE-FISH.

(A-a) A small ( $\leq 5 \mu\text{m}$  WBC) CD44v6<sup>+</sup>/Vim<sup>+</sup>/CD31<sup>-</sup> haploid CTC ( ${}_3\text{CTC}^{\text{mono}}$ ). (A-b) A small CD44v6<sup>+</sup>/Vim<sup>-</sup>/CD31<sup>-</sup> triploid CTC ( ${}_3\text{CTC}^{\text{tri}}$ ). (A-c) A small CD44v6<sup>+</sup>/Vim<sup>-</sup>/CD31<sup>-</sup> tetraploid CTC ( ${}_3\text{CTC}^{\text{tetra}}$ ). (A-d) A large ( $>5 \mu\text{m}$ ) CD44v6<sup>+</sup>/Vim<sup>-</sup>/CD31<sup>-</sup> multiploid ( $\geq$  pentasomy 8) CTC ( ${}_L\text{CTC}^{\text{multi}}$ ). (A-e) A CTC cluster consisting of three CD44v6<sup>+</sup>/Vim<sup>-</sup>/CD31<sup>-</sup> multiploid null cells. (A-f) A CTC-WBC cluster comprising a large CD44v6<sup>+</sup>/Vim<sup>-</sup>/CD31<sup>-</sup> multiploid CTC and two CD45<sup>+</sup> WBCs. (B-a) A large CD44v6<sup>+</sup>/Vim<sup>+</sup>/CD31<sup>+</sup> diploid CTEC ( ${}_L\text{CTEC}^{\text{di}}$ ). (B-b) A large CD44v6<sup>+</sup>/Vim<sup>+</sup>/CD31<sup>+</sup> triploid CTEC ( ${}_L\text{CTEC}^{\text{tri}}$ ). (B-c) A large CD44v6<sup>+</sup>/Vim<sup>-</sup>/CD31<sup>+</sup> tetraploid CTEC ( ${}_L\text{CTEC}^{\text{tetra}}$ ). (B-d) A large CD44v6<sup>+</sup>/Vim<sup>-</sup>/CD31<sup>+</sup> multiploid CTEC ( ${}_L\text{CTEC}^{\text{multi}}$ ). (B-e) A homotypic CTEC cluster of two small CD44v6<sup>+</sup>/Vim<sup>-</sup>/CD31<sup>+</sup> multiploid null cells. (B-f) A heterotypic CTC-WBC cluster consisting of a large CD44v6<sup>+</sup>/Vim<sup>-</sup>/CD31<sup>+</sup> multiploid CTEC and two CD45<sup>+</sup> WBCs. Bars, 5  $\mu\text{m}$ .

CD44v6<sup>+</sup>/Vim<sup>-</sup>/CD31<sup>+</sup> tetraploid ( $t_0$ CTEC<sup>tetra</sup>, Fig. 3Bc), and CD44v6<sup>+</sup>/Vim<sup>-</sup>/CD31<sup>+</sup> multiploid ( $t_0$ CTEC<sup>multi</sup>, Fig. 3Bd) cells. Additionally, a homotypic CTEC cluster of two small CD44v6<sup>+</sup>/Vim<sup>-</sup>/CD31<sup>+</sup> multiploid null cells (Fig. 3Be) and a heterotypic CTC-WBC cluster consisting of a large CD44v6<sup>+</sup>/Vim<sup>-</sup>/CD31<sup>+</sup> multiploid CTEC and two CD45<sup>+</sup> WBCs (Fig. 3Bf) are displayed. Given the high morphologic, phenotypic, and karyotypic tumor cell heterogeneity, we set out to analyze how carcinoma cell subtypes evolve in the peripheral circulation under therapeutic pressure.

### 3.3. Patients' characteristics and categorical analysis of CTCs and CTECs

A total of 120 eligible SCLC patients were prospectively enrolled, including 55 LD- and 65 ED-SCLC (Supplementary Table S1). Correlations of CTCs, CTECs, and their CD44v6-expressing subpopulations with patients' clinical characteristics were investigated. Quantification at baseline ( $t_0$ ) revealed the presence of CTCs in 113 out of 120 (94.16%) patients and CTECs in 100 out of 120 patients (83.33%). Both CTCs  $\geq 18$  and CTECs  $\geq 8$  each per 6 ml blood were found to significantly correlate with liver metastases ( $***p < 0.001$ ,  $*p = 0.024$ , respectively) (Supplementary Table S2). Twenty out of 120 (16.67%) patients had CD44v6<sup>+</sup> CTCs detected, and 35 out of 120 (29.16%) patients harbored CD44v6<sup>+</sup> CTECs at baseline (Supplementary Table S3). Patients with positive detection of CD44v6<sup>+</sup> CTCs or CD44v6<sup>+</sup> CTECs showed significantly increased hepatic metastasis than those harboring none of CD44v6<sup>+</sup> CTCs or CD44v6<sup>+</sup> CTECs ( $**p = 0.002$ ,  $*p = 0.024$ , respectively; Supplementary Table S3). Obtained results suggested that the acquisition of a CD44v6<sup>+</sup> phenotype may be associated with more aggressive cell behavior. Consequently, numbers of aneuploid CTCs and CTECs were assessed in a longitudinal manner in SCLC patients under therapy. Median numbers of CTCs were 6 ( $t_0$ , blue, IQR 3–17.75), 7 ( $t_1$ , purple, IQR 4–16), and 7.5 ( $t_2$ , purple, IQR 5–17.25), while median numbers of CTECs over time were 3 ( $t_0$ , blue, IQR 1–7.75), 2 ( $t_1$ , purple, IQR 0–7), and 1.5 ( $t_2$ , purple, IQR 0–4), respectively (Fig. 4Aa-b). As most SCLC patients were exceptionally responsive to initial treatment, the bulky tumor mass commonly shrank distinctly after chemotherapy administration, potentially along with a release of tumor cells in blood circulation. Accordingly, we observed that CTC numbers were significantly higher at  $t_1$  and  $t_2$  than  $t_0$  ( $t_0$  vs.  $t_2$ ,  $*p = 0.048$ ;  $t_1$  vs.  $t_2$ ,  $*p = 0.040$ ), whereas CTEC numbers decreased under therapy, but differences did not reach statistical significance (Fig. 4Aa-b). The increase in CTCs and a concurrent reduction of CTECs were further corroborated by CTEC/CTC ratios at the indicated time intervals. The median value of the CTEC/CTC ratio was 0.5 ( $t_0$ , IQR 0.07–1.00), 0.27 ( $t_1$ , IQR 0–0.86), and 0.16 ( $t_2$ , IQR 0–0.40), respectively, and the CTEC/CTC ratio was significantly higher at  $t_0$  than at  $t_1$  or  $t_2$  ( $t_0$  vs.  $t_1$ ,  $**p = 0.003$ ;  $t_0$  vs.  $t_2$ ,  $**p = 0.003$ ;  $t_1$  vs.  $t_2$ ,  $*p = 0.030$ , Fig. 4Ac-d). Obtained results suggested that CTCs and CTECs constitute a pair of viable, real-time cellular circulating tumor biomarkers.

We further investigated karyotype variations in CTCs, CTECs, and their CD44v6 subtypes along with treatment administration. CTCs, CTECs, and CD44v6<sup>+</sup> CTECs showed similar proportions of Chr8 haploid, diploid, triploid, tetraploid, and multiploidy cells during therapy (Fig. 4Ba, c-e). However, Chr8 copy numbers in post-treatment CD44v6<sup>+</sup> CTCs shifted towards multiploidy compared to trisomy 8 in pre-treatment CD44v6<sup>+</sup> CTCs (Fig. 4Bb, e). It has been reported that the degree of aneuploidy is proportionally correlated with tumor's malignancy grade, moreover, the chromosomal instability contributes to the evolution of therapeutic resistance. Thus, the acquired increase in multiploidy in CD44v6<sup>+</sup> CTC upon treatment might reflect the burden of circulating neoplastic cells resistant to therapeutic regimens in SCLC patients.

### 3.4. Correlation of CTC variation trends with patients' survival

Using the X-tile software, the optimal CTC cut-off value to stratify

pre-treatment patients with respect to overall survival was 17 (Supplementary Figs. S2A–E). Subgroup analysis demonstrated that baseline CTCs had statistical prognostic significance in ED-SCLC ( $*p = 0.001$  for PFS and  $**p = 0.004$  for OS, Supplementary Fig. S2F, f), but not for LD-SCLC patients ( $p = 0.700$  for PFS and  $p = 0.087$  for OS, Supplementary Fig. S2Fb, e).

Patients were further classified into low-baseline (0–17) and high-baseline cohorts ( $\geq 18$ ), respectively. Comparison of CTCs between prior to therapy and post-treatment groups was performed on 95 patients who were available for the longitudinal assessment. All 95 patients were further stratified into four sub-cohorts according to both baseline quantity of CTCs ( $t_0$ ) and variation trends throughout therapy ( $t_{1-2}$ ) (Fig. 5A). Patients were classified into low-baseline counts and descending numbers of CTCs upon treatment (LB-DESC,  $n = 23$ , including LD-SCLC  $n = 13$ , and ED-SCLC  $n = 10$ ), low-baseline ascending (LB-ASC,  $n = 50$ , including LD-SCLC  $n = 24$ , ED-SCLC  $n = 26$ ), high-baseline descending (HB-DESC,  $n = 21$ , including LD-SCLC  $n = 10$ , ED-SCLC  $n = 11$ ), and high-baseline ascending cohorts (HB-ASC,  $n = 1$ , which was LD-SCLC  $n = 1$ ) (Fig. 5B). The longitudinal variation of CTC numbers in each patient was analyzed and results were graphically depicted as the log value of  $\Delta t = (t_{1 \text{ or } 2} - t_0)$  (i.e., subtraction value between last time point to  $t_0$ ) (Fig. 5A).

Dynamic changes of CTC numbers in each sub-cohort across three time points were respectively investigated. Median values of CTCs in the LB-DESC cohort were 8 ( $t_0$ , blue, Min 1/Max 17), 3 ( $t_1$ , purple, Min 0/Max 126), and 2.5 CTCs ( $t_2$ , purple, Min 1/Max 7), respectively (Fig. 5Ca). Differences in CTC numbers were statistically significant among three time points ( $*p = 0.014$ ). Analysis of subgroups classified upon disease stages was performed. A significant downward variation trend was observed on LD-SCLC patients but not on ED-SCLC patients in the LB-DESC cohort (Fig. 5Cb-c  $*p = 0.019$ ,  $p = 0.219$ , respectively). In the LB-ASC cohort, median values of CTCs were 3 ( $t_0$ , blue, Min 0/Max 12), 7 ( $t_1$ , purple, Min 0/Max 89), and 17 cells ( $t_2$ , purple, Min 5/Max 60), and differences were statistically significant ( $***p < 0.001$ ; Fig. 5Cd). Both, LD- and ED-SCLC patients displayed significant upward quantitative variations in CTC numbers following treatment ( $***p < 0.001$ ,  $***p < 0.001$ , respectively; Fig. 5Ce-f). Within the HB-DESC cohort, differences in median numbers of CTCs were statistically significant and reduced from baseline 29 ( $t_0$ , blue, Min 18/Max 554), to 15 ( $t_1$ , purple, Min 0/Max 92), then down to 9 cells ( $t_2$ , purple, Min 1/Max 14) ( $***p < 0.001$ ; Fig. 5Cg). Similar analysis revealed that downward quantitative variations at the indicated time intervals reached statistical significance in both LD- and ED-SCLC patients ( $**p = 0.004$ ,  $**p = 0.007$ , respectively; Fig. 5Ch-i).

Correlation of CTC variation trends with survival was analyzed utilizing Kaplan-Meier curves. Patients in the LB-DESC cohort showed a significantly longer median OS (mOS) than patients in LB-ASC or HB-DESC cohorts (N/A vs 14.53 m vs 14.20 m,  $**p = 0.001$ , Log rank for trend test; Fig. 5Da). Additional subgroup analysis revealed that CTC variation trends were of statistical prognostic significance in both LD-SCLC (N/A vs N/A vs 15.33 months,  $*p = 0.0498$ , log rank for trend test; Fig. 5Db) and ED-SCLC patients (N/A vs 11.07 vs 9.47 months,  $*p = 0.013$ , Log rank for trend test; Fig. 5Dc). Low baseline quantity and decreased CTC numbers following therapy were significantly associated with prolonged OS.

### 3.5. CTC and CTEC-relevant variables correlate with metastasis, treatment response and prognosis in SCLC patients

Previous studies revealed difficulties in terms of adequately predicting treatment response or prognosis by CTCs alone. Multivariable analysis of relevant CTC and CTEC-relevant variables may help provide more useful information. CTC and CTEC-relevant variables, including CTC variation trends, CD44v6<sup>+</sup> CTCs ( $t_0$ ), post-therapeutic CD44v6<sup>+</sup> CTCs ( $t_{1-2}$ ), CTEC/CTC ratio ( $t_0$ ), CTM ( $t_0$ ) and CTC-WBC clusters ( $t_0$ ) along with disease stage were implemented in a neural network-based

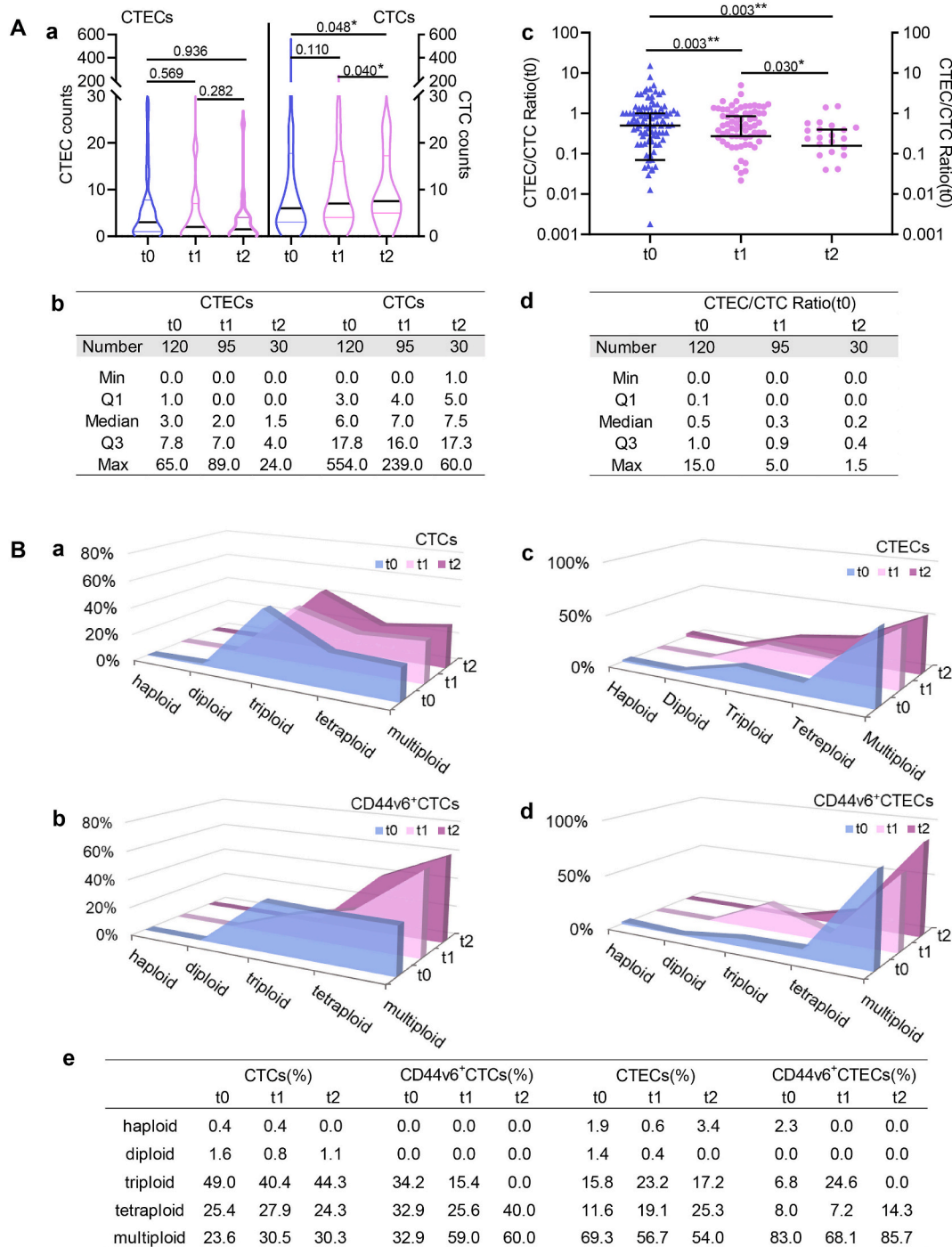
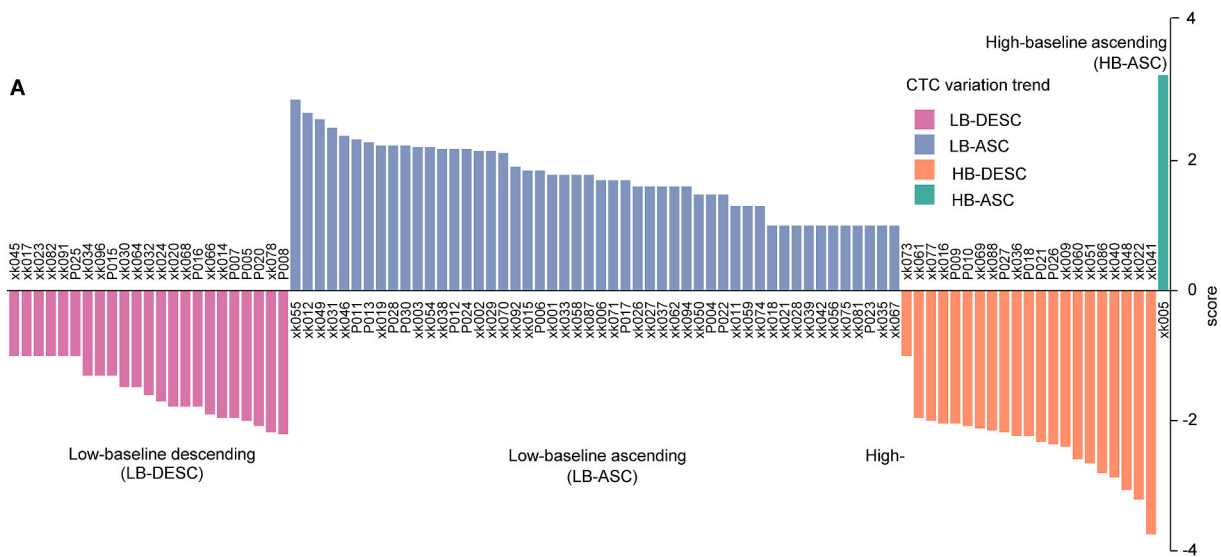


**Fig. 4. Quantitative and karyotypic analysis of CD31<sup>-</sup> CTCs and CD31<sup>+</sup> CTECs longitudinally detected in SCLC patients.**

A. Quantitative analysis of aneuploid CTCs and CTECs detected in overall pre- and post-treatment SCLC patients is demonstrated in (Aa, b). Analysis of CTECs/CTCs ratio in pre- and post-treatment SCLC patients is revealed in (Ac, d). B. Comprehensive analysis of diverse karyotypes of CTCs and CTECs at the designated baseline (t<sub>0</sub>), 2 therapy cycles (t<sub>1</sub>) and 4–6 therapy cycles (t<sub>2</sub>). Comparing the proportion variation of Chr8 copy numbers from t<sub>0</sub> to t<sub>2</sub> in CTCs (Ba), CTECs (Bc), and CD44v6<sup>+</sup> CTCs (Bd), only CD44v6<sup>+</sup> CTCs show a significantly increased proportion of multiploidy at t<sub>1-2</sub> compared to t<sub>0</sub> (Bb).

algorithm model (Fig. 6A). CD44v6<sup>+</sup> CTCs (t<sub>1-2</sub>) showed the highest impact (normalized importance) within the model. Correlations between “variables (normalized importance ≥20%) and clinical factors” in LD-SCLC patients were depicted and analyzed in the heatmap in Fig. 6Ba. The incidence of distant metastasis at the time of disease progression in CD44v6<sup>+</sup> CTCs (t<sub>1-2</sub>) patients was significantly higher than those without CD44v6<sup>+</sup> CTCs (t<sub>1-2</sub>) (\*\*p < 0.001, Table 1). It has been noted that brain metastasis was more frequent in patients with positive detection of CD44v6<sup>+</sup> CTCs (t<sub>1-2</sub>) than in those harboring none

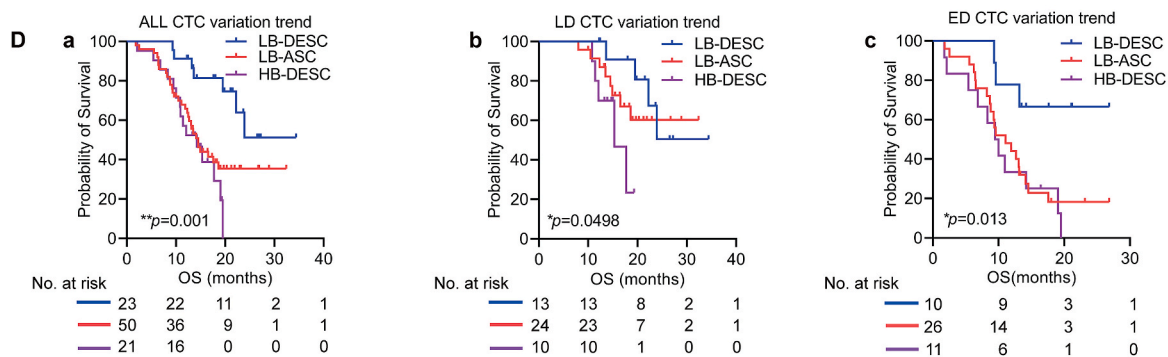
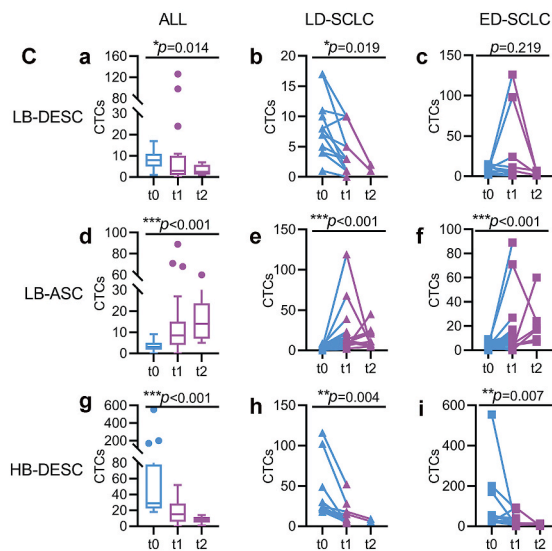
of CD44v6<sup>+</sup> CTCs (t<sub>1-2</sub>) (\*\*p < 0.001, Table 1). CD44v6<sup>+</sup> CTCs (t<sub>1-2</sub>) were also correlated with decreased disease control rate (DCR, \*p = 0.025, Table 1) and the poor survival (\*p = 0.045, Table 1), which demonstrated unique advantages of longitudinal detection of CD44v6<sup>+</sup> CTCs with respect to monitoring treatment response in real-time. Meanwhile, distant metastases, especially brain metastasis, developed more frequently in patients with CTEC/CTC ratio (t<sub>0</sub>) ≥0.5 than in those with CTEC/CTC (t<sub>0</sub>) ratio <0.5 (\*p = 0.047, Table 1). CTEC/CTC ratio (t<sub>0</sub>) ≥0.5 was also correlated with decreased DCR and the poor survival



**B**

	ALL		LD-SCLC		ED-SCLC	
	Patients N	Samples n	Patients N	Samples n	Patients N	Samples n
Low-baseline descending (LB-DESC)	23	54	13	29	10	25
Low-baseline ascending (LB-ASC)	50	116	24	58	26	58
High-baseline descending (HB-DESC)	21	48	10	22	11	26
High-baseline ascending (HB-ASC)	1	2	1	2	0	0
<b>Total</b>	<b>95</b>	<b>220</b>	<b>48</b>	<b>111</b>	<b>47</b>	<b>109</b>

Low-baseline: CTCs 0-17; High-baseline: CTCs ≥18; descending: CTCs  $\Delta t(t1 \text{ or } 2 - t0) \leq 0$ ; ascending: CTCs  $\Delta t(t1 \text{ or } 2 - t0) > 0$



(caption on next page)

**Fig. 5. Clinical significance of subcategorized CTC variation trends in SCLC patients.**

(A) A total of 95 patients are categorized into four cohorts according to the baseline CTC number and CTC variation trends: the low baseline-descending cohort (LB-DESC): baseline CTCs( $t_0$ ) = 0–17, post-therapeutic CTC number is lower than that at baseline ( $\Delta t \leq 0$ ,  $\Delta t = t_{1 \text{ or } 2} - t_0$ ); the low baseline-ascending cohort (LB-ASC): CTCs( $t_0$ ) = 0–17, post-therapeutic CTC number is higher than that at baseline ( $\Delta t > 0$ ); the high baseline-descending cohort (HB-DESC): CTCs( $t_0$ )  $\geq 18$ ,  $\Delta t \leq 0$ ; and the high baseline-ascending cohort (HB-ASC): CTCs( $t_0$ )  $\geq 18$ ,  $\Delta t > 0$ . Detailed longitudinal variation of CTC quantity in each patient is graphically depicted by the log value of  $\Delta t$  and summarized in (B). (C) Quantitative variation of CTCs in the indicated cohort of patients throughout therapy. (Ca) In LB-DESC cohort, the median values of CTCs were 8 (purple, Min0/Max 126,  $t_1$ ), and 3 cells (purple, Min1/Max 7,  $t_2$ ), respectively, the difference is statistically significant ( $*p = 0.014$ ). Subgroup analysis reveals a significant downward variation trend in LD (Cb) but not for ED patients (Cc) ( $*p = 0.019$ ,  $p = 0.219$ , respectively). (Cd) In LB-ASC cohort, the median values of CTCs were 3 (blue, Min0/Max12,  $t_0$ ), 7 (purple, Min0/Max 89,  $t_1$ ), and 17 cells (purple, Min5/Max 60,  $t_2$ ) with a significant statistical significance ( $***p < 0.001$ ), both LD (Ce) and ED (Cf) SCLC patients display statistically significant upward quantitative variations ( $***p < 0.001$ ,  $***p < 0.001$ , respectively). (Cg) In HB-DESC cohort, median values of CTCs were 29 (blue, Min18/Max 554,  $t_0$ ), 15 (purple, Min0/Max 92,  $t_1$ ), and 9 cells (purple, Min1/Max 14,  $t_2$ ) ( $***p < 0.001$ ). Downward quantitative variations reached a significant statistical significance in both LD (Ch) and ED (Ci) SCLC patients ( $**p = 0.004$ ,  $**p = 0.007$ , respectively). (D) Clinical significance of subcategorized CTC variation trends in SCLC patients. (Da) OS curve is depicted based on CTC variation trends at the full data set. Patients in low baseline-descending cohort (blue) show a significantly longer mOS than those in low baseline-ascending (red) and high baseline-descending cohorts (purple) (N/A vs 14.53 vs 14.20 months,  $*p = 0.001$ , Log rank for trend test). Analysis of diverse CTC variation trends in subcategorized cohorts indicates the dynamic monitoring of CTCs in LD- and ED-SCLC subjects indicates that LB-DESC cohort in both categories have a longer OS, showing LD subjects in (Db), N/A for LB-DESC vs N/A for LB-ASC vs 15.33 months for HB-DESC,  $p = 0.050$ ); and ED patients in (Dc), N/A for LB-DESC vs 11.07 months for LB-ASC vs 9.47 months for HB-DESC,  $*p = 0.013$ ). N/A: not available.

( $*p = 0.017$ ;  $*p = 0.031$ , Table 1). Moreover, patients with combined CD44v6<sup>+</sup> CTCs ( $t_{1-2}$ ) and CTEC/CTC ratio ( $t_0$ )  $\geq 0.5$  were more likely to develop distant metastasis, especially brain metastasis, and exhibited decreased DCR and poor survival ( $*p = 0.012$ ;  $*p = 0.027$ ;  $**p = 0.003$ ;  $*p = 0.034$  respectively, Table 1). In addition, CD44v6<sup>+</sup> CTCs ( $t_{1-2}$ ) and CTC-WBC clusters ( $t_0$ ) were associated with brain metastasis, decreased DCR, and poor survival in LD-SCLC patients ( $*p = 0.022$ ;  $*p = 0.047$ ;  $**p = 0.009$ , Table 1). The interplay between CTCs and CTECs may be a key determinant in developing brain metastasis and therapeutic resistance in LD-SCLC patients. A similar analysis was conducted in ED-SCLC patients (Supplementary Fig. S3), however, neither single nor combined variables was correlated with clinical factors in ED-SCLC patients.

In our study, all patients with brain metastasis at the time of disease progression were analyzed. Correlation between variables and brain metastasis was depicted in the heatmap (Fig. 6Bb). The incidence of brain metastasis at the time of disease progression was significantly higher in patients possessing CD44v6<sup>+</sup> CTCs ( $t_{1-2}$ ) than in those without CD44v6<sup>+</sup> CTCs ( $t_{1-2}$ ) ( $**p = 0.009$ , Fig. 6Bc). Furthermore, CD44v6<sup>+</sup> CTCs ( $t_{1-2}$ ) combining with CTEC/CTC ratio ( $t_0$ ) or CTC-WBC cluster ( $t_0$ ) were also correlated with brain metastasis ( $*p = 0.025$ ;  $*p = 0.039$ , respectively, Fig. 6Bc). Brain metastasis is common in SCLC at diagnosis or amid disease progression. Identification of above brain metastasis risk factors may help guide more ideal individualized management of SCLC.

### 3.6. Longitudinal detection of CD44v6<sup>+</sup> CTCs independently predicts poor prognosis in SCLC patients

Among 95 patients available for the longitudinal CTC detection, six patients had constant CD44v6<sup>+</sup> CTCs from baseline to post-therapy ( $t_0$ ,  $t_2$ ), and 15 subjects displayed post-therapeutic CD44v6<sup>+</sup> CTCs. Moreover, 62 patients showed unchanged CD44v6<sup>-</sup> CTCs status during treatment, and 12 patients had CD44v6<sup>+</sup> CTCs eliminated following treatment administration.

Till the last follow-up, 70 out of 120 SCLC patients died. The mOS was 13.5 months. Univariate analysis revealed that patients possessing post-therapeutic CD44v6<sup>+</sup> CTCs ( $t_{1-2}$ ) had a median PFS (mPFS) of 5.4 months, which was statistically shorter than 9.6 months for patients without CD44v6<sup>+</sup> CTCs ( $t_{1-2}$ ) (Fig. 6Ca). Similarly, patients harboring CD44v6<sup>+</sup> CTCs ( $t_{1-2}$ ) had an mOS of 13.1 months, which was significantly shorter than 19.0 months for patients without CD44v6<sup>+</sup> CTCs ( $t_{1-2}$ ) ( $*p = 0.011$ , log-rank test; Fig. 6Da). Subgroup analysis revealed that dynamic detection of CD44v6<sup>+</sup> CTCs was significantly correlated with both PFS and OS in LD-SCLC patients ( $*p = 0.004$  and  $*p = 0.018$ , log-rank test; Fig. 6Cb, Db). As for ED-SCLC patients, dynamic monitoring of CD44v6<sup>+</sup> CTCs was able to effectively predict PFS ( $*p = 0.024$ , Fig. 6Cc) but not OS ( $p = 0.264$ , Fig. 6Dc), showing that longitudinal detection of CD44v6<sup>+</sup> CTCs was correlated with reduced PFS in both LD and ED

patients but only predicted poor OS in LD-SCLC patients.

Clinical characteristics, along with CTC and CTEC-relevant variables possessing statistical significance in univariate analysis, were included in a multivariate Cox proportional hazard model (Table 2). Longitudinal detection of CD44v6<sup>+</sup> CTCs and disease stage functioned as independent prognostic factors associated with PFS ( $*p = 0.001$ ;  $***p < 0.001$ , respectively). Meanwhile, longitudinal positive detection of CD44v6<sup>+</sup> CTCs, CTC-WBC clusters ( $t_0$ ), and disease stage were confirmed as independent risk factors for OS ( $*p = 0.021$ ;  $**p = 0.001$ ;  $***p < 0.001$ , respectively, Table 2). These results indicated that similar to disease stages, CD44v6<sup>+</sup> CTCs detected amid therapy are the independent prognostic factor for both PFS and OS.

## 4. Discussion

Rapidly acquired treatment resistance and emergence of distant metastases are major causes of mortality in SCLC patients [40,41]. The ability to promptly characterize patients at-risk for developing treatment resistance and/or metastases is in urgent need to enable more appropriate clinical management of SCLC [42].

It has been reported that a high CTC count is associated with poor prognosis of SCLC [43,44], and conversion from an unfavorable baseline CTC level to a favorable follow-up CTC level greatly improves survival of SCLC patients [45,46]. The present study showed that the low baseline-descending cohort (LB-DESC) of patients exhibited significantly prolonged survival compared with those in low baseline-ascending (LB-ASC) and high baseline-descending cohorts (HB-DESC), implying that baseline and post-therapeutic CTC quantities should be collectively observed to timely index the prognosis of patients.

Aneuploidy, a state of chromosomal imbalance, is a hallmark of cancer cells [47–49]. Alterations of chr8, including amplification at 8q24 harboring the *c-Myc* oncogene and high GSR gene activity, are one of the most common chromosomal abnormalities in lung cancer [50,51]. Though it has been documented that chromosome aneuploidy in neoplastic cells can induce genetic instability and that the degree of aneuploidy is positively correlated with the malignancy grade of tumor cells [48,52,53], few studies have investigated the landscape of karyotype heterogeneity of rare circulating cells in SCLC.

Increasing evidence has highlighted that intratumor heterogeneity and cells exhibiting stem-like properties have a critical role in tumor initiation, treatment resistance, and disease progression in various cancers [54–58]. However, stem cell relevant studies have been limited by the rarity of tumor tissues, particularly for SCLC.

It has been reported that the stemness phenotype is intimately interconnected with EMT and involved in a broad range of oncogenic processes including cell invasion and metastasis [59–62]. To investigate whether CD44v6 contributes to metastasis, *in vitro* functional assays of

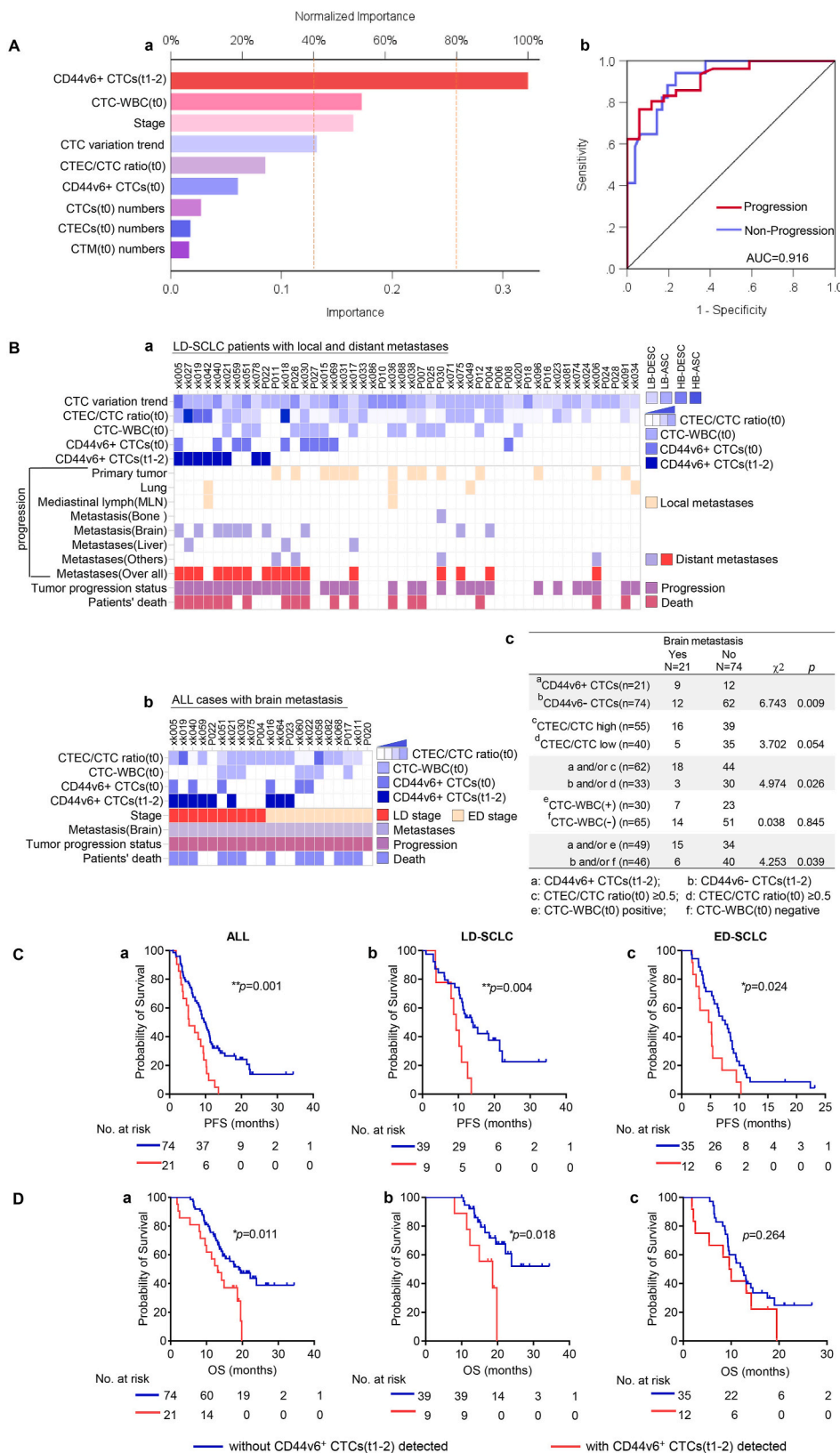


**Fig. 6. Correlation of CD31<sup>-</sup> CTC and CD31<sup>+</sup> CTEC-related variables with cancer metastasis and treatment response in SCLC.**

(Aa-b) CTCs and CTECs variables including CTCs variation trends, CD44v6<sup>+</sup> CTCs (t<sub>0</sub>), CD44v6<sup>+</sup> CTCs (t<sub>1-2</sub>), CTECs/CTCs (t<sub>0</sub>) ratio, CTM(t<sub>0</sub>) and CTC-WBC(t<sub>0</sub>) cluster along with disease stage were evaluated based on the neural network algorithm. (Ba) The association between CTCs and CTECs variables with normalized importance ≥ 20% and metastasis, treatment efficiency and survival exhibited by heatmap. (Bb) The association between CTCs and CTECs variables and brain metastasis exhibited by heatmap. (Bc) Correlation analysis of CD31<sup>-</sup> CTCs and CD31<sup>+</sup> CTECs variables with brain metastasis. (C) PFS analysis: (Ca) For overall patients possessing acquired post-therapeutic CD44v6<sup>+</sup> CTCs (t<sub>1-2</sub>, red) has a mPFS significantly shorter than those without post-treatment CD44v6<sup>+</sup> CTCs (t<sub>1-2</sub>, blue) (5.40 vs 9.60 months, \*\**p* < 0.001). (Cb) LD-SCLC: positive detection of post-therapeutic CD44v6<sup>+</sup> CTCs significantly correlates with a shorter PFS (9.37 vs 13.73 months, \*\**p* = 0.004). (Cc) ED-SCLC: CD44v6<sup>+</sup> CTCs may well predict PFS (4.70 vs 7.57 months, \**p* = 0.024). (D) OS analysis: (Da) All patients harboring post-therapeutic CD44v6<sup>+</sup> CTCs (t<sub>1-2</sub>, red) show a mOS significantly shorter than those with post-treatment CD44v6<sup>+</sup> CTCs (t<sub>1-2</sub>, blue) (13.13 vs 19.30 months, \**p* = 0.011). (Db) LD-SCLC: post-therapeutic CD44v6<sup>+</sup> CTCs significantly correlate with the inferior OS (18.60 vs N/A, \**p* = 0.018). (Dc) ED-SCLC: no significant correlation is observed between longitudinally detected CD44v6<sup>+</sup> CTCs with OS (9.80 vs 12.47 months, *p* = 0.264).

CD44v6 in two SCLC cell lines were performed. Obtained data illustrated that overexpression of CD44v6 promoted the invasion and metastasis of SCLC cells, overexpression of CD44v6 down-regulated epithelial marker *E-cadherin* and up-regulated mesenchymal marker vimentin. Therefore, CD44v6 may promote cell invasion and metastasis

via activation of EMT. In the current study, SE-iFISH [63–65] was utilized to thoroughly investigate the clinical significance of aneuploid CD31<sup>-</sup> CTCs and CD31<sup>+</sup> CTECs expressing the stemness marker CD44v6 in SCLC patients. Obtained results demonstrated that positive detection of both CD44v6<sup>+</sup> CTCs and CD44v6<sup>+</sup> CTECs in pre-treatment patients

**Table 1**  
Correlation of CD31<sup>-</sup> CTCs and CD31<sup>+</sup> CTECs with distant metastases (including brain metastasis) and disease progression in LD-SCLC patients.

	Distant metastases		$\chi^2$	<i>p</i>	Brain metastasis		$\chi^2$	<i>p</i>	PD	SD + PR	$\chi^2$	<i>p</i>	Death	Survival	$\chi^2$	<i>p</i>					
	Yes	No			Yes	No											N =	N =	N =	N =	N = 30
	N = 17	N = 31			N = 10	N = 38											33	15	18	30	
<sup>a</sup> CD44v6 <sup>+</sup> CTCs (n = 9)	8	1	13.850	0.000	6	3	14.110	0.000	9	0	5.035	0.025	6	3	4.021	0.045					
<sup>b</sup> CD44v6 <sup>-</sup> CTCs (n = 39)	9	30			4	35			24	15			12	27							
CTCs <18 (n = 10)	4	6	0.116	0.341	3	7	0.644	0.422	6	4	0.450	0.502	6	4	2.728	0.099					
CTCs ≥18 (n = 38)	13	25			7	31			27	11			12	26							
<sup>c</sup> CTEC/CTC high (n = 25)	11	14	1.680	0.195	8	17	3.945	0.047	21	4	5.648	0.017	13	12	4.680	0.031					
<sup>d</sup> CTEC/CTC low (n = 23)	6	17			2	21			12	11			5	18							
a and/or c (n = 28)	14	14	6.248	0.012	10	18	9.023	0.027	24	4	9.002	0.003	14	14	4.480	0.034					
b and/or d (n = 20)	3	17			0	20			9	11			4	16							
<sup>e</sup> CTC-WBC <sup>+</sup> (t <sub>0</sub> )s (n = 15)	6	9	0.109	0.741	3	12	0.200	0.654	11	4	0.213	0.644	8	7	2.333	0.127					
<sup>f</sup> CTC-WBC <sup>-</sup> (t <sub>0</sub> ) (n = 33)	11	22			7	26			22	11			10	23							
a and/or e (n = 23)	13	10	3.273	0.070	8	15	5.210	0.023	19	4	3.948	0.047	13	10	6.817	0.009					
b and/or f (n = 25)	4	11			2	23			14	11			5	20							

<sup>a</sup> CD44v6<sup>+</sup> CTCs(t<sub>1-2</sub>).  
<sup>b</sup> CD44v6<sup>-</sup> CTCs(t<sub>1-2</sub>).  
<sup>c</sup> CTEC/CTC ratio (t<sub>0</sub>) ≥0.5.  
<sup>d</sup> CTEC/CTC ratio (t<sub>0</sub>) <0.5.  
<sup>e</sup> CTC-WBC<sup>+</sup> (t<sub>0</sub>).  
<sup>f</sup> CTC-WBC<sup>-</sup> (t<sub>0</sub>).

**Table 2**  
Analysis of univariate and multivariate Cox proportional hazard model.

Variables	Univariate analysis				Multivariate analysis			
	PFS		OS		PFS		OS	
	HR (95% CI)	<i>p</i>	HR (95% CI)	<i>P</i>	HR (95% CI)	<i>p</i>	HR (95% CI)	<i>p</i>
Age	1.1 (0.7–1.8)	0.676	17 (1.0–3.0)	0.063	–	–	–	–
≥70 vs. <70								
Gender	1.6 (1.0–2.5)	0.07	2.0 (1.0–3.7)	0.036	–	–	1.1 (0.3–4.4)	0.847
male vs. female								
PS 1–2 vs. 0	1.3 (0.7–2.2)	0.431	2.1 (1.0–4.6)	0.056	–	–	–	–
Smoking history	1.8 (1.1–3.1)	0.023	1.9 (1.0–3.8)	0.047	1.4 (0.8–2.6)	0.253	1.8 (0.4–1.7)	0.399
Yes vs. No								
Disease stage	2.8 (1.8–4.2)	0.000	3.6 (2.1–6.0)	0.000	3.0 (1.9–4.8)	0.000	3.9 (2.1–7.3)	0.000
extensive vs. limited								
CTC-WBC	1.3 (0.9–2.0)	0.195	1.8 (1.1–2.8)	0.018	–	–	2.9 (1.6–5.5)	0.001
Pos vs. Neg								
CTC variation trend	–	0.713	–	0.005	–	–	–	0.123
LB-DESC vs. LB-ASC vs. HB-DESC								
CD44v6 <sup>+/f</sup> CTCs								
CD44v6 <sup>-</sup> (t <sub>1-2</sub> )	2.4 (1.4–4.0)	0.001	2.1 (1.2–3.9)	0.011	2.4 (1.4–4.0)	0.001	2.2 (1.1–4.4)	0.021
CD44v6 <sup>+</sup> (t <sub>1-2</sub> )								

correlated with liver metastasis. Mechanismly, CD44v6 engages in the processes of metastasis by interacting with hyaluronic acid (HA) or osteopontin [66]. HA-CD44v6 interaction supports the colonization of metastatic cells by activating RTK associated signaling pathway [67]. Moreover, the interaction of hematopoietic proteoglycan serglycin with CD44 promotes lung cancer aggressiveness and liver colonization [68].

Further karyotype analysis in our study indicated that, comparing to the most pre-treatment CD44v6<sup>+</sup> CTCs bearing trisomy 8, a significantly increased proportion of multiploid (≥ pentasomy 8) CD44v6<sup>+</sup> CTCs was observed in post-treatment patients. Given that the degree of aneuploidy is proportional to the grade of malignancy of neoplastic cells [69,70], the specific subtype of multiploid CD44v6<sup>+</sup> CTCs may potentially

represent a more aggressive drug-resistant CTC subtype with greater metastatic ability, thus contributing to a worse prognosis.

Brain metastasis is a common but fatal event for cancer patients [71–73]. In SCLC, approximately 10% of patients demonstrating brain metastasis at the time of initial diagnosis and an additional 40–50% subsequently developing brain metastasis as a result of tumor progression [74,75]. A recent study indicated that CD44 and CD74 expression on CTCs is associated with brain metastasis in breast cancer [76]. Our results revealed that the constant existence of post-therapeutic CD44v6<sup>+</sup> CTCs ( $t_{0-2}$ ) may also participate in the process of brain metastasis in SCLC patients. Additional comprehensive analysis of CTCs and CTECs demonstrated that the ratio of CTEC/CTC is significantly correlated with both brain metastasis and treatment efficiency in LD-SCLC patients, suggesting that aneuploid CD31<sup>-</sup> CTCs and their counterpart CD31<sup>+</sup> CTECs may function as a pair of cellular circulating tumor biomarkers throughout disease progression.

Whether and how the prognosticator CD44v6<sup>+</sup> CTCs correlated with patients' prognosis was further investigated in this study. It has been published that CD44<sup>+</sup> CTCs in either blood or bone marrow in gastric cancer were associated with poor survival [34]. Moreover, pre-operative pancreatic ductal adenocarcinoma (PDAC) patients harboring CD44<sup>+</sup> CTECs exhibited shorter DFS following radical surgery [36]. Results obtained in this study illustrated similar findings to previously reported positive association of CD44<sup>+</sup> CTCs with inferior prognosis. Univariate analysis demonstrated that longitudinal detection of CD44v6<sup>+</sup> CTCs can predict SCLC patients' poor prognosis, especially for LD-SCLC patients. Multivariate analysis further validated the detection of CD44v6<sup>+</sup> CTCs as an independent risk factor of inferior prognosis, and longitudinal detection of CD44v6<sup>+</sup> CTCs may allow for the non-invasive monitoring of disease progression and patients' survival. Our results confirmed the crucial implication of CD44v6<sup>+</sup>/CD31<sup>-</sup> CTCs as a promising biomarker for predicting therapeutic resistance and clinical outcome in SCLC patients and may facilitate patient stratification in future clinical trials.

In clinical practice, LD-SCLC is a potentially curable disease with long-term survival of 15–20% [77,78], whereas for ED-SCLC patients, combination chemotherapy may prolong survival and improve quality of life; however, long-term survival is rare [79,80]. Since treatment goals differ for LD- and ED-SCLC patients, i.e., cure versus palliation, ideal biomarkers are necessary for more appropriate risk stratification of SCLC, particularly for LD subjects who are likely to achieve a favorable long-term outcome. The present study demonstrated that post-therapeutic CTC variation trends, CD44v6<sup>+</sup> CTCs ( $t_0$ ,  $t_{1-2}$ ), and CTEC/CTC ratio ( $t_0$ ) are either uniquely or collectively correlated with treatment response, distant metastasis, and survival in LD-SCLC patients, suggesting that comprehensive analysis of CTC and CTEC-relevant variables may assist identification of specified LD-SCLC patients who would benefit most from aggressive concurrent chemoradiation with curative intent. Moreover, co-detection and molecular characterization of diverse subtypes of aneuploid CTCs and CTECs may help in more appropriate personalized treatment decision making, selection of patients who are likely to benefit from curative surgery, and drug development for the potentially curable LD-SCLC.

In summary, our study for the first time demonstrates that longitudinally detected CD44v6<sup>+</sup>/CD31<sup>-</sup> CTCs, an independent prognosticator for inferior PFS and OS, correlate with SCLC treatment resistance and distant metastases, particularly brain metastasis. Comprehensive analyses of subcategorized CTCs and CTECs as well as their CD44v6<sup>+</sup> subtypes in conjunction with the current image-based staging system enable novel clinical stratification and improve prognostic prediction of SCLC patients, particularly for LD-SCLC.

#### CRediT authorship contribution statement

**Ying Wang:** Writing – original draft, Software, Resources, Methodology, Investigation, Formal analysis, Data curation. **Lina Zhang:** Writing – original draft, Software, Resources, Methodology,

Investigation, Formal analysis, Data curation. **Jinjing Tan:** Writing – original draft, Software, Resources, Methodology, Investigation, Formal analysis. **Zhiyun Zhang:** Resources, Investigation, Data curation. **Yanxia Liu:** Resources, Investigation, Data curation. **Xingsheng Hu:** Resources, Investigation. **Baohua Lu:** Resources, Investigation. **Yuan Gao:** Resources, Investigation. **Li Tong:** Resources, Investigation. **Zan Liu:** Resources, Investigation. **Hongxia Zhang:** Resources, Investigation. **Peter Ping Lin:** Writing – review & editing, Visualization, Validation. **Baolan Li:** Validation. **Olivier Gires:** Writing – review & editing, Visualization, Validation, Supervision, Project administration, Methodology, Conceptualization. **Tongmei Zhang:** Writing – review & editing, Visualization, Validation, Supervision, Project administration, Methodology, Funding acquisition, Conceptualization.

#### Declaration of competing interest

Dr. Peter P. Lin is the president at Cytelligen. None of the authors has Cytelligen's stock. No additional COI to be declared.

#### Acknowledgements

Authors thank staff at Beijing Chest Hospital, Cytointelligen (China Medical City, Taizhou, Jiangsu, China), and Cytelligen (San Diego, CA, USA) for providing support to this study. Authors also thank patients and their families for participating in this study.

This work was supported by Beijing Municipal Science and Technology Commission [grant number Z211100002921013]. Tongzhou Lianggao Talents Project [grant number YH201920]. Tongzhou District Science and Technology Committee Project to TZ [grant number KJ2020CX010].

#### Appendix A. Supplementary data

Supplementary data to this article can be found online at <https://doi.org/10.1016/j.canlet.2023.216337>.

#### References

- [1] R.L. Siegel, et al., Cancer statistics, 2021, *CA A Cancer J. Clin.* 71 (1) (2021) 7–33.
- [2] X. Yin, et al., Small cell lung cancer transformation: from pathogenesis to treatment, *Semin. Cancer Biol.* 86 (Pt 2) (2022) 595–606.
- [3] N. Zhang, et al., PARP inhibitor plus radiotherapy reshapes an inflamed tumor microenvironment that sensitizes small cell lung cancer to the anti-PD-1 immunotherapy, *Cancer Lett.* 545 (2022), 215852.
- [4] S. Taromi, et al., Enhanced AC133-specific CAR T cell therapy induces durable remissions in mice with metastatic small cell lung cancer, *Cancer Lett.* 538 (2022), 215697.
- [5] S. Wang, et al., Development and validation of a nomogram prognostic model for SCLC patients, *J. Thorac. Oncol.* 13 (9) (2018) 1338–1348.
- [6] J.B. Yu, et al., Surveillance epidemiology and end results evaluation of the role of surgery for stage I small cell lung cancer, *J. Thorac. Oncol.* 5 (2) (2010) 215–219.
- [7] Z. Megyesfalvi, et al., Expression patterns and prognostic relevance of subtype-specific transcription factors in surgically resected small-cell lung cancer: an international multicenter study, *J. Pathol.* 257 (5) (2022) 674–686.
- [8] A.K.P. Ganti, et al., Small cell lung cancer, version 2.2022, NCCN clinical practice guidelines in oncology, *J. Natl. Compr. Cancer Netw.* 19 (12) (2021) 1441–1464.
- [9] Y. Tian, et al., Single-cell transcriptomic profiling reveals the tumor heterogeneity of small-cell lung cancer, *Signal Transduct. Targeted Ther.* 7 (1) (2022) 346.
- [10] A. Sun, et al., Guideline for the initial management of small cell lung cancer (limited and extensive stage) and the role of thoracic radiotherapy and first-line chemotherapy, *Clin. Oncol.* 30 (10) (2018) 658–666.
- [11] G.S. Jones, et al., A systematic review of survival following anti-cancer treatment for small cell lung cancer, *Lung Cancer* 141 (2020) 44–55.
- [12] K. Kang, et al., Tackling the current dilemma of immunotherapy in extensive-stage small cell lung cancer: a promising strategy of combining with radiotherapy, *Cancer Lett.* 565 (2023), 216239.
- [13] Y. Tian, et al., Radiation therapy for extensive-stage small-cell lung cancer in the era of immunotherapy, *Cancer Lett.* 541 (2022), 215719.
- [14] C. Liu, et al., Blood-based liquid biopsy: insights into early detection and clinical management of lung cancer, *Cancer Lett.* 524 (2022) 91–102.
- [15] Z. Lin, et al., Exosomal circRNAs in cancer: implications for therapy resistance and biomarkers, *Cancer Lett.* 566 (2023), 216245.
- [16] H. Huang, et al., Blood protein biomarkers in lung cancer, *Cancer Lett.* 551 (2022), 215886.

- [17] Z.R. Reichert, et al., Prognostic value of plasma circulating tumor DNA fraction across four common cancer types: a real-world outcomes study, *Ann. Oncol.* 34 (1) (2023) 111–120.
- [18] M.J. Poellmann, et al., Circulating tumor cell abundance in head and neck squamous cell carcinoma decreases with successful chemoradiation and cetuximab treatment, *Cancer Lett.* 562 (2023), 216187.
- [19] M. Wang, et al., Gastric cancer cell-derived extracellular vesicles disrupt endothelial integrity and promote metastasis, *Cancer Lett.* 545 (2022), 215827.
- [20] P.P. Lin, et al., Comprehensive in situ co-detection of aneuploid circulating endothelial and tumor cells, *Sci. Rep.* 7 (1) (2017) 9789.
- [21] P.P. Lin, Aneuploid circulating tumor-derived endothelial cell (CTEC): a novel versatile player in tumor neovascularization and cancer metastasis, *Cells* 9 (6) (2020).
- [22] K. Hida, M. Klagsbrun, A new perspective on tumor endothelial cells: unexpected chromosome and centrosome abnormalities, *Cancer Res.* 65 (7) (2005) 2507–2510.
- [23] C. Lu, et al., Gene alterations identified by expression profiling in tumor-associated endothelial cells from invasive ovarian carcinoma, *Cancer Res.* 67 (4) (2007) 1757–1768.
- [24] H. Cheng, et al., Combined detection and subclass characteristics analysis of CTCs and CTECs by SE-IFISH in ovarian cancer, *Chin. J. Cancer Res.* 33 (2) (2021) 256–270.
- [25] Y. Lei, et al., Combined detection of aneuploid circulating tumor-derived endothelial cells and circulating tumor cells may improve diagnosis of early stage non-small-cell lung cancer, *Clin. Transl. Med.* 10 (3) (2020) e128.
- [26] G. Dong, et al., Cancer-associated fibroblasts: key criminals of tumor pre-metastatic niche, *Cancer Lett.* 566 (2023), 216234.
- [27] R.Y. Tay, et al., Prognostic value of circulating tumour cells in limited-stage small-cell lung cancer: analysis of the concurrent once-daily versus twice-daily radiotherapy (CONVERT) randomised controlled trial, *Ann. Oncol.* 30 (7) (2019) 1114–1120.
- [28] J.M. Hou, et al., Clinical significance and molecular characteristics of circulating tumor cells and circulating tumor microemboli in patients with small-cell lung cancer, *J. Clin. Oncol.* 30 (5) (2012) 525–532.
- [29] M. Hassan Mesrati, et al., CD44: a multifunctional mediator of cancer progression, *Biomolecules* 11 (12) (2021).
- [30] W. Chen, et al., CD44v6+ hepatocellular carcinoma cells maintain stemness properties through met/cJun/nanog signaling, *Stem Cell. Int.* 2022 (2022), 5853707.
- [31] Q. Cheng, et al., LGR4 cooperates with PrPc to endow the stemness of colorectal cancer stem cells contributing to tumorigenesis and liver metastasis, *Cancer Lett.* 540 (2022), 215725.
- [32] L. Zhou, et al., HULC targets the IGF1R-PI3K-AKT axis in trans to promote breast cancer metastasis and cisplatin resistance, *Cancer Lett.* 548 (2022), 215861.
- [33] M. Li, et al., Stem cell-like circulating tumor cells indicate poor prognosis in gastric cancer, *BioMed Res. Int.* 2014 (2014), 981261.
- [34] A. Szczepanik, et al., CD44(+) cyokeratin-positive tumor cells in blood and bone marrow are associated with poor prognosis of patients with gastric cancer, *Gastric Cancer* 22 (2) (2019) 264–272.
- [35] K.E. Poruk, et al., Circulating tumor cells expressing markers of tumor-initiating cells predict poor survival and cancer recurrence in patients with pancreatic ductal adenocarcinoma, *Clin. Cancer Res.* 23 (11) (2017) 2681–2690.
- [36] C. Xing, et al., CD44+ circulating tumor endothelial cells indicate poor prognosis in pancreatic ductal adenocarcinoma after radical surgery: a pilot study, *Cancer Manag. Res.* 13 (2021) 4417–4431.
- [37] T. Zhang, et al., Role of aneuploid circulating tumor cells and CD31(+) circulating tumor endothelial cells in predicting and monitoring anti-angiogenic therapy efficacy in advanced NSCLC, *Mol. Oncol.* 15 (11) (2021) 2891–2909.
- [38] Y. Wang, et al., Vimentin expression in circulating tumor cells (CTCs) associated with liver metastases predicts poor progression-free survival in patients with advanced lung cancer, *J. Cancer Res. Clin. Oncol.* 145 (12) (2019) 2911–2920.
- [39] L. Zhang, et al., PD-L1(+) aneuploid circulating tumor endothelial cells (CTECs) exhibit resistance to the checkpoint blockade immunotherapy in advanced NSCLC patients, *Cancer Lett.* 469 (2020) 355–366.
- [40] B.H. Herzog, S. Devarakonda, R. Govindan, Overcoming chemotherapy resistance in SCLC, *J. Thorac. Oncol.* 16 (12) (2021) 2002–2015.
- [41] J. Ko, M.M. Winslow, J. Sage, Mechanisms of small cell lung cancer metastasis, *EMBO Mol. Med.* 13 (1) (2021), e13122.
- [42] S. Tariq, et al., Update 2021: management of small cell lung cancer, *Lung* 199 (6) (2021) 579–587.
- [43] A. De Luca, et al., Promising role of circulating tumor cells in the management of SCLC, *Cancers* 13 (9) (2021).
- [44] V. Foy, et al., EPAC-lung: European pooled analysis of the prognostic value of circulating tumour cells in small cell lung cancer, *Transl. Lung Cancer Res.* 10 (4) (2021) 1653–1665.
- [45] T. Naito, et al., Prognostic impact of circulating tumor cells in patients with small cell lung cancer, *J. Thorac. Oncol.* 7 (3) (2012) 512–519.
- [46] P.O. Bendahl, M. Belting, E. Gezelius, Longitudinal assessment of circulating tumor cells and outcome in small cell lung cancer: a sub-study of RASTEN-A randomized trial with low molecular weight heparin, *Cancers* 15 (12) (2023).
- [47] H.E. Danielsen, M. Pradhan, M. Novelli, Revisiting tumour aneuploidy - the place of ploidy assessment in the molecular era, *Nat. Rev. Clin. Oncol.* 13 (5) (2016) 291–304.
- [48] K.H. Stopsack, et al., Aneuploidy drives lethal progression in prostate cancer, *Proc. Natl. Acad. Sci. U.S.A.* 116 (23) (2019) 11390–11395.
- [49] S.F. Yeung, et al., TEC kinase stabilizes PLK4 to promote liver cancer metastasis, *Cancer Lett.* 524 (2022) 70–81.
- [50] A.N. Seo, et al., Clinicopathologic and prognostic significance of c-MYC copy number gain in lung adenocarcinomas, *Br. J. Cancer* 110 (11) (2014) 2688–2699.
- [51] M. Baity, et al., Glutathione reductase (GSR) gene deletion and chromosome 8 aneuploidy in primary lung cancers detected by fluorescence in situ hybridization, *Am. J. Cancer Res.* 9 (6) (2019) 1201–1211.
- [52] A.M. Taylor, et al., Genomic and functional approaches to understanding cancer aneuploidy, *Cancer Cell* 33 (4) (2018) 676–689.e3.
- [53] U. Kronenwett, et al., Improved grading of breast adenocarcinomas based on genomic instability, *Cancer Res.* 64 (3) (2004) 904–909.
- [54] J. Codony-Servat, A. Verlicchi, R. Rosell, Cancer stem cells in small cell lung cancer, *Transl. Lung Cancer Res.* 5 (1) (2016) 16–25.
- [55] C.J. O'Conor, et al., Cancer stem cells in triple-negative breast cancer: a potential target and prognostic marker, *Biomarkers Med.* 12 (7) (2018) 813–820.
- [56] Z. Jahanafrooz, et al., Colon cancer therapy by focusing on colon cancer stem cells and their tumor microenvironment, *J. Cell. Physiol.* 235 (5) (2020) 4153–4166.
- [57] F. Guo, et al., Natural killer cell therapy targeting cancer stem cells: old wine in a new bottle, *Cancer Lett.* 570 (2023), 216328.
- [58] H. Dianat-Moghadam, et al., Engaging stemness improves cancer immunotherapy, *Cancer Lett.* 554 (2023), 216007.
- [59] D.R. Pattabiraman, R.A. Weinberg, Tackling the cancer stem cells - what challenges do they pose? *Nat. Rev. Drug Discov.* 13 (7) (2014) 497–512.
- [60] J. He, et al., *Helicobacter pylori* infection induces stem cell-like properties in Correa cascade of gastric cancer, *Cancer Lett.* 542 (2022), 215764.
- [61] Y. Liang, et al., CD146 interaction with integrin  $\beta 1$  activates LATS1-YAP signaling and induces radiation-resistance in breast cancer cells, *Cancer Lett.* 546 (2022), 215856.
- [62] G. Rigillo, et al., The NF-Y splicing signature controls hybrid EMT and ECM-related pathways to promote aggressiveness of colon cancer, *Cancer Lett.* 567 (2023), 216262.
- [63] Y. Li, et al., Evolutionary expression of HER2 conferred by chromosome aneuploidy on circulating gastric cancer cells contributes to developing targeted and chemotherapeutic resistance, *Clin. Cancer Res.* 24 (21) (2018) 5261–5271.
- [64] L. Wang, et al., Quantified postsurgical small cell size CTCs and EpCAM(+) circulating tumor stem cells with cytogenetic abnormalities in hepatocellular carcinoma patients determine cancer relapse, *Cancer Lett.* 412 (2018) 99–107.
- [65] Y. Chen, et al., Dysregulated KRAS gene-signaling axis and abnormal chromatin remodeling drive therapeutic resistance in heterogeneous-sized circulating tumor cells in gastric cancer patients, *Cancer Lett.* 517 (2021) 78–87.
- [66] L. Ma, L. Dong, P. Chang, CD44v6 engages in colorectal cancer progression, *Cell Death Dis.* 10 (1) (2019) 30.
- [67] V. Orian-Rousseau, J. Sleeman, CD44 is a multidomain signaling platform that integrates extracellular matrix cues with growth factor and cytokine signals, *Adv. Cancer Res.* 123 (2014) 231–254.
- [68] J.Y. Guo, et al., Serglycin in tumor microenvironment promotes non-small cell lung cancer aggressiveness in a CD44-dependent manner, *Oncogene* 36 (17) (2017) 2457–2471.
- [69] D.J. Gordon, B. Resio, D. Pellman, Causes and consequences of aneuploidy in cancer, *Nat. Rev. Genet.* 13 (3) (2012) 189–203.
- [70] C.D. Steele, et al., Signatures of copy number alterations in human cancer, *Nature* 606 (7916) (2022) 984–991.
- [71] A. Tyagi, S.Y. Wu, K. Watabe, Metabolism in the progression and metastasis of brain tumors, *Cancer Lett.* 539 (2022), 215713.
- [72] W. Xu, et al., Extracellular vesicle-derived LINC00482 induces microglial M2 polarization to facilitate brain metastasis of NSCLC, *Cancer Lett.* 561 (2023), 216146.
- [73] S.R. Sirkisoon, et al., Breast cancer extracellular vesicles-derived miR-1290 activates astrocytes in the brain metastatic microenvironment via the FOXA2→CNTF axis to promote progression of brain metastases, *Cancer Lett.* 540 (2022), 215726.
- [74] C.M. Rudin, et al., Small-cell lung cancer, *Nat. Rev. Dis. Prim.* 7 (1) (2021) 3.
- [75] R. Rittberg, et al., Treatment and prevention of brain metastases in small cell lung cancer, *Am. J. Clin. Oncol.* 44 (12) (2021) 629–638.
- [76] D. Loreth, et al., CD74 and CD44 expression on CTCs in cancer patients with brain metastasis, *Int. J. Mol. Sci.* 22 (13) (2021).
- [77] A.T. Turrisi 3rd, et al., Twice-daily compared with once-daily thoracic radiotherapy in limited small-cell lung cancer treated concurrently with cisplatin and etoposide, *N. Engl. J. Med.* 340 (4) (1999) 265–271.
- [78] K. Doshita, et al., Long-term survival data of patients with limited disease small cell lung cancer: a retrospective analysis, *Invest. N. Drugs* 40 (2) (2022) 411–419.
- [79] L.A. Byers, C.M. Rudin, Small cell lung cancer: where do we go from here? *Cancer* 121 (5) (2015) 664–672.
- [80] E. Caliman, et al., Challenges in the treatment of small cell lung cancer in the era of immunotherapy and molecular classification, *Lung Cancer* 175 (2023) 88–100.